

Published in final edited form as:

*Angew Chem Int Ed Engl.* 2012 June 18; 51(25): 6074–6092. doi:10.1002/anie.201200063.

## Recent Advances in Azaborine Chemistry

**Patrick G. Campbell**

Department of Chemistry University of Oregon 1253 University of Oregon, Eugene OR, 97403-1253, USA Fax: (+1) 541 346-0487

**Dr. Adam J. V. Marwitz**

Department of Chemistry University of Calgary Calgary, AB, Canada

**Prof. Dr. Shih-Yuan Liu**

Department of Chemistry University of Oregon 1253 University of Oregon, Eugene OR, 97403-1253, USA Fax: (+1) 541 346-0487 [lsy@uoregon.edu](mailto:lsy@uoregon.edu)

### Abstract

The chemistry of organoboron compounds has been primarily dominated by their use as powerful reagents in synthetic organic chemistry. Recently, the incorporation of boron as part of a functional target structure has emerged as a useful way to generate diversity in organic compounds. A commonly applied strategy is the replacement of a CC unit with its isoelectronic BN unit. In particular, the BN/CC isosterism of the ubiquitous arene motif has undergone a renaissance in the past decade. The parent molecule of the 1,2-dihydro-1,2-azaborine family has now been isolated. New mono- and polycyclic BN heterocycles have been synthesized for potential use in biomedical and materials science applications. This review is a tribute to Dewar's first synthesis of a monocyclic 1,2-dihydro-1,2-azaborine 50 years ago and discusses recent advances in the synthesis and characterization of carbon(C)-boron(B)-nitrogen(N)-containing heterocycles.

### Keywords

boron; nitrogen; aromaticity; heterocycles; azaborines

## 1. Introduction

Boron has been playing a crucial role in the field of chemistry. William Lipscomb (1976),<sup>[1]</sup> Herbert C. Brown (1979),<sup>[2]</sup> and more recently, Akira Suzuki (2010)<sup>[3]</sup> have each been recognized with the Nobel Prize for their contributions in boron chemistry. Today, boron-containing compounds represent a powerful tool for synthetic chemists.<sup>[4–7]</sup> In most targeted synthetic applications, however, the element boron typically is not part of the final functional structure. Because of boron's unique electronic structure and its ability to form covalent bonds with carbon, the inclusion of boron in organic structures has recently received significant attention in biomedical research<sup>[8]</sup> and in optoelectronic materials applications.<sup>[9]</sup>

An emerging strategy of incorporation of boron in organic structures is the substitution of a CC bond with an isoelectronic and isosteric BN unit (BN/CC isosterism). The isoelectronic nature between the BN and CC bonding arises from the fact that boron has three valence electrons and nitrogen has five valence electrons, and consequently, a BN unit has the same

valence electron count (i.e., 8 valence electrons) as a corresponding CC unit in which each carbon contributes 4 valence electrons (Figure 1).

Despite the same total valence electron count, differences in molecular properties can be expected when replacing an organic CC unit with the corresponding BN unit. The comparison between ethane vs. ammonia borane (AB) and ethene vs. aminoborane nicely illustrates this point (Figure 2). Ethane is a volatile gas under standard conditions (bp:  $-89$  °C); it has no effective dipole moment;<sup>[10]</sup> the CC bond dissociation energy (BDE) is 90.1 kcal/mol.<sup>[11]</sup> In contrast, ammonia borane is a solid under standard conditions (mp: 104 °C); it has a strong dipole moment of 5.2 D;<sup>[12]</sup> its bond dissociation energy (27.2 kcal/mol) is significantly smaller than that of ethane.<sup>[13]</sup> Similar to ethane, the unsaturated ethene is an isolable volatile gas under standard conditions (bp:  $-104$  °C); due to symmetry of the molecule, its dipole moment is also zero;<sup>[10]</sup> the BDE is 174.1 kcal/mol of which 109.1 kcal/mol is due to  $\sigma$  bond contribution and 65 kcal/mol is due to  $\pi$  contribution.<sup>[11,14]</sup> On the other hand, the BN analogue of ethene, aminoborane, is a reactive molecule with a strong tendency to polymerize/oligomerize under standard conditions. The parent aminoborane monomer has been characterized in the gas phase by microwave spectroscopy, which indicated an ethene-like planar structure.<sup>[15]</sup> The BN BDE in aminoborane is 139.7 kcal/mol of which 109.8 kcal/mol is attributed to the  $\sigma$  bond and only 29.9 kcal/mol to the  $\pi$  contribution.<sup>[13]</sup> Aminoborane has a dipole moment of 1.84 D,<sup>[15]</sup> which is significantly less than that of ammonia borane.

It has been postulated that the reduced dipole moment in aminoborane (vs. AB) is a result of opposing forces present in the two resonance structures representing aminoborane.<sup>[16]</sup> Figure 3 illustrates that the dipole that is due to nitrogen's higher electronegativity (vs. boron) in the left resonance structure opposes the dipole that is due to the formal charges in the right resonance structure as a result of  $\pi$ -bonding.

Among the three possible variants to replace a CC with a BN (Figure 1), the “ $sp^2$ ”-type BN/CC isosterism associated with conjugated aromatic systems has received the most attention. This is because of the ubiquity and wide utility of arene-containing compounds and the increased stability of the corresponding BN-containing isosteres compared to “ $sp^3$ ”-type BN isosteres. The potential to dramatically increase the diversity of aromatic structures and tune their electronic properties through BN/CC isosterism have led to a burgeoning interest in this area. The first example of BN/CC isosterism of an arene was reported by Alfred Stock in 1926<sup>[17]</sup> with the synthesis of borazine (c- $B_3N_3H_6$ ), the inorganic counterpart to the quintessential aromatic compound benzene (c- $C_6H_6$ ). Similar to benzene, borazine continues to receive significant attention in pure and applied chemistry.<sup>[18–23]</sup> Although commonly referred to as the “inorganic benzene”, borazine's aromatic character remains controversial to date.<sup>[24–27]</sup>

Since the pioneering contribution by Stock, the isoelectronic relationship between B–N and C=C has led to the development of aromatic systems *partially* substituted with boron and nitrogen (carbon-boron-nitrogen (CBN) heterocycles). Though somewhat limited in scope, the first major achievements in the synthesis of CBN heterocycles took place in the 1960s. After several decades of diminished activity in the field, modern synthetic protocols have prompted a resurgence in the study of CBN heterocycles since the turn of the millennium.

This review is a summary of the advances made since the last comprehensive review on the subject by Piers and coworkers in early 2009,<sup>[28]</sup> and is not an exhaustive history of CBN heterocycle chemistry. For the sake of brevity, and in recognition of the 50<sup>th</sup> Anniversary of Dewar's first synthesis of a monocyclic 1,2-dihydro-1,2-azaborine, we will focus on aromatic 6-membered heterocycles that are isoelectronic with benzene and which contain

only one BN substitution. This particular substitution pattern results in three possible isomers, referred to throughout this text as 1,2-azaborine **A**, 1,3-azaborine **B** and 1,4-azaborine **C** (Figure 4). Examples of each isomer have now been synthesized and will be discussed here, along with polycyclic compounds containing either the 1,2- or 1,4-azaborine core (1,3-azaborine-containing polycyclic compounds are as yet unknown). Important early work that has been covered in prior reviews will be discussed briefly to provide context for recent developments. The chemistry of boron dipyrrole (BODIPY)<sup>[29]</sup> and phthalocyanine dyes<sup>[30]</sup> as well as substitution with BN units in cluster compounds and graphitic materials,<sup>[28]</sup> are beyond the scope of this work. This review is organized by research group and will explore how the targeted applications of the products, along with the unique methodologies employed in their synthesis, have contributed to the present wealth and diversity of BN-containing compounds.

## 2. Pioneering Work

In 1958 Dewar reported the synthesis of the first singly B-N substituted aromatic compounds, 9,10-azaboraphenanthrenes.<sup>[31]</sup> The reaction of 2-phenylaniline with  $\text{BCl}_3$  and  $\text{AlCl}_3$  gave 9,10-azaboraphenanthrene **2** (Scheme 1), presumably through the Friedel-Crafts cyclization of intermediate **1**. The substitution of various nucleophiles at the reactive B-Cl unit of **2** allowed for the synthesis of several BN-phenanthrene derivatives **3–6**. The isoelectronic relationship between BN-phenanthrene **6** and its carbon analog was explored via UV-Vis spectroscopy. The spectrum of **6** resembles very closely that of phenanthrene in the position of the main absorption bands. However, an increase in the intensity of the  $\alpha$ -band was observed, an effect that was attributed to removing the molecular orbital degeneracy in the BN-substituted heterocycle. The reactivity of BN-phenanthrene was explored in depth. It was found to undergo electrophilic aromatic substitution regioselectively at the 6 and 8 positions, depending on the electrophile.<sup>[32–35]</sup> Deprotonation/substitution was possible at the nitrogen position, and tuning the electronics of the nitrogen substituent was found to have an effect on the electronics of the heterocycle as a whole. For example, the *N*-acyl substituted compound **8** rapidly oxidized when exposed to air, in sharp contrast to other derivatives that were quite air-stable (Scheme 2).<sup>[36]</sup>

The first BN-naphthalene was synthesized by Dewar and coworkers in 1959.<sup>[37]</sup> The reaction of 2-aminostyrene with phenylboron dichloride led to the direct formation of 2-phenyl-1,2-azaboranaphthalene **9** (Scheme 3). BN-naphthalenes **9**, **11–13** were reported to be unreactive toward strong base and  $\text{KMnO}_4$ , signifying a high degree of resonance stabilization.<sup>[38]</sup> Further evidence of resonance stabilization in BN-naphthalene was provided via the comparative reactivity of partially reduced heterocycle **14**, which reacted immediately with acid or base to give ring-opened **15** (Scheme 4).<sup>[39]</sup> In contrast, BN-naphthalene **11** was completely stable to hydrolysis, even upon heating.

Dewar and coworkers also reported the first electrophilic aromatic substitution reactions of BN-naphthalene (Scheme 5).<sup>[40]</sup> The halogenation of 1,2-azaboranaphthalene **12** with  $\text{Cl}_2$  and  $\text{Br}_2$  produced a mixture of C3-substituted products **16** and **17** and ring-opened side-products **18** and **19**. The structural assignments of **16** and **17** were confirmed by an independent synthesis of these compounds.

The aqueous stability of 1,2-azaboranaphthalenes made them attractive targets for the biological incorporation of boron (e. g., for cancer treatment using boron neutron capture therapy).<sup>[41]</sup> However, 1,2-azaboranaphthalene was found to be water-insoluble, limiting its use in biological systems. Dewar and coworkers were able to improve the solubility of 1,2-azaboranaphthalenes by functionalizing **12** at the nitrogen position (Scheme 6).<sup>[41]</sup>

Dewar and coworkers also synthesized the [9,10] isomer of BN-naphthalene (Scheme 7).<sup>[42]</sup> Treatment of di-3-butenylamine with trimethylamine borane formed bicycle **28**. Subsequent oxidation with Pd/C at high temperature afforded **29**, which was characterized by <sup>1</sup>H and <sup>11</sup>B NMR spectroscopy as well as mass spectrometry. Notably, the bridgehead-substituted BN-naphthalene **29** was found to have the same odor as naphthalene, which is a qualitative yet astounding testament to the chemical similarity between BN heterocycles and their all-carbon analogs.

The EAS reactivity of **29** was demonstrated, via H/D exchange, to occur at the carbons alpha to boron.<sup>[37]</sup> Dewar and coworkers therefore sought to synthesize the 10,11-azaboraphenalenium cation **30** via substitution at the alpha carbons of **29**.<sup>[43]</sup> The reaction of **29** with malonaldehyde bis-diethylacetal and CF<sub>3</sub>CO<sub>2</sub>H led to the formation of an intense purple solution attributed to the formation of **30** (characterized by <sup>1</sup>H NMR spectroscopy and mass spectrometry) that was stable at -78 °C but decomposed at higher temperatures (Scheme 8). The <sup>1</sup>H NMR spectrum of the BN-phenalenium cation was similar to that of its carbon analog.

Dewar and White pioneered the first syntheses of monocyclic 1,2-azaborine derivatives independently in the early 1960s. In 1962, Dewar and coworkers used a desulfurization strategy from BN-benzothiophene **31** to generate highly-substituted 1,2-azaborine **32** (Scheme 9).<sup>[44]</sup> Compound **32** was resistant to degradation under prolonged exposure to both acid and base in ethanol. Acid/base stability and the inertness of the 1,2-azaborine double bonds toward Raney nickel are indications of the aromatic stability of the 1,2-azaborine core. In 1963, White reported the synthesis of 1-H-2-phenyl-1,2-azaborine **34** via Pd-catalyzed dehydrogenation from saturated heterocycle **33** (Scheme 10).<sup>[45]</sup>

In 1967, Dewar and coworkers attempted the first synthesis of the parent 1,2-Dihydro-1,2-azaborine using a hydroborationoxidation protocol, but were unsuccessful (Scheme 11).<sup>[46]</sup> They concluded that, "Borazarene [1,2-Dihydro-1,2-azaborine] therefore seems to be a very reactive and chemically unstable system, prone to polymerization and other reactions..." In fact, multiple attempts to isolate the parent 1,2-Dihydro-1,2-azaborine from BN-triphenylene **36** were unsuccessful.

Other pioneers of BN-heterocycle chemistry include Polivka and coworkers who followed a similar route to Dewar's BN-naphthalene synthesis to generate 1,2-azaboracyclohexane **37** from dimethylaminobut-3-ene (Scheme 12), however no attempts were made to aromatize this compound.<sup>[47,48]</sup>

Goubeau and coworkers used a secondary butenyl amine (as in White's earlier work) to form the cyclohexene analog **38** via hydroboration (Scheme 13).<sup>[49]</sup> Dehydrogenation with Pd/Al<sub>2</sub>O<sub>3</sub> provided the first *B*-H substituted 1,2-azaborine **39**, which was characterized by mass spectrometry.<sup>[50]</sup>

Gronowitz and coworkers synthesized a series of BN-benzothiophenes, which upon desulfurization yielded the first examples of monocyclic 1,2-azaborines substituted at C4 and/or C5 (Scheme 14).<sup>[51-53]</sup>

The pioneering efforts of these groups hinted at the potential of azaborine-containing compounds as arene mimics in a diverse variety of structural motifs. However, early development was hampered by the limited material characterization capabilities of the times and harsh synthetic conditions incompatible with many functional groups. Modern synthetic protocols and instrumentation have enabled a new generation of chemists to pick up where

Dewar, White and others left off, and take azaborine chemistry into uncharted and exciting territory.

### 3. The Ashe Group – University of Michigan

The Ashe group achieved a breakthrough in the mild synthesis of monocyclic 1,2-azaborines in 2000 and sparked renewed interest in the field of aromatic BN-heterocycles. Previous syntheses relied on desulfurization or dehydrogenation at extreme temperatures as discussed above, but Ashe and coworkers developed a ring-closing metathesis/oxidation protocol that enabled mild and efficient formation of 1,2-azaborines (Scheme 15).<sup>[54]</sup> Transmetalation of allyltributyltin with  $\text{BCl}_3$  generated allylboron dichloride **45** *in situ*. Condensation with allylethylamine produced bisallyl aminoborane **46**. The addition of PhLi led to the displacement of chloride from the labile *B*-Cl bond to give *B*-Ph aminoborane **47** in good yield. Ring-closing metathesis with Grubbs' first generation catalyst formed 1,2-azaborine precursor **48** featuring an olefin at the 4-position. The oxidation to 1,2-azaborine **49** was accomplished in good yield using 2,3-dichloro-5,6-dicyano-1,4-benzoquinone (DDQ) at 35 °C.

A year later, Ashe and coworkers explored a ring-expansion route to 1,2-azaborines from the 1,2-azaborolide heterocycle, which is formally isoelectronic with the ubiquitous cyclopentadienide (Cp) anion (Scheme 16).<sup>[55]</sup> Ring-closing metathesis from *B*-vinyl aminoboranes **50** provided heterocycles **51**, which were deprotonated to give 1,2-azaborolides **52**. The reaction of **52** with  $\text{CH}_2\text{Cl}_2$  and lithium diisopropylamide (LDA) (the Katz reaction) gave 1,2-azaborines **53a-c**. A deuterium labeling study suggested that the initial attack of chlorocarbene occurs at the C3 position of **52c**. Carbene insertion into the B-C bond leads to a 3-deuterio isomer of **53c** via carbene **54**. Deuterium incorporation at this position rules out initial substitution at C5.

The Ashe group has explored the reactivity of 1,2-azaborines extensively, especially with regard to their transition metal chemistry. They have synthesized  $\eta^6$  piano-stool chromium and molybdenum complexes,<sup>[55]</sup> ruthenium sandwich compounds,<sup>[56]</sup> as well as  $\eta^1$  zirconium complexes bound at the deprotonated azaborine nitrogen.<sup>[57]</sup> They developed a new route to 5- and 6-membered ring-fused bicyclic 1,2-azaborines.<sup>[58]</sup> They also demonstrated the first electrophilic aromatic substitution reactions of a monocyclic 1,2-azaborine.<sup>[59]</sup> The majority of the work the Ashe group has done in this field was described in detail in Piers' 2009 review<sup>[28]</sup> and we will not repeat it here. However, since then, two new reports have emerged from Ashe and coworkers regarding BN-aromatic compounds.

In one, Ashe and coworkers investigated the haptotropic migration of *B*-phenyl 1,2-azaboranaphthalene **9** in  $\text{Cr}(\text{CO})_3$  piano-stool complexes (Scheme 17).<sup>[60]</sup> The complexation of **9** with  $\text{Cr}(\text{CO})_3$  was envisioned to occur at the benzenoid, 1,2-azaborine, or even the boron-substituted phenyl ring. In fact,  $\eta^6$  binding of the benzenoid ring was observed under mild heating to form complex **55**. At higher temperatures, however, a shift of chromium complexation to the boron-substituted phenyl ring occurred forming complex **56**, with no evidence for the formation of complex **57**. In fact, even when **56** was deprotonated with LiTMP to generate complex **58**, no haptotropic migration to **59** was observed; instead complex **58** was prone to thermal degradation. These data indicate that the heterocyclic ring of BN-naphthalene is a poor ligand for transition metals relative to monocyclic 1,2-azaborines.

Ashe and coworkers strategized that removal of the competitive *B*-phenyl binding site would allow for the binding of transition metals to the heterocyclic fragment of BN-naphthalene. To that end, *B*-methyl 1,2-azaboranaphthalene **12** was treated with



(MeCN)<sub>3</sub>Cr(CO)<sub>3</sub> to give complex **60** (Scheme 18). Though no complexation to the heterocyclic fragment was observed, deprotonation of **60** with potassium hexamethyldisilazide provided **61**, which increased the electron-richness of the 1,2-azaborine heterocycle. Upon heating, complex **61** underwent a haptotropic migration to afford the desired anionic complex **62** in which chromium is  $\eta^6$ -bound to the heterocyclic ring. Methylation of **62** presumably led to complex **63**, however the coordination of the neutral heterocyclic fragment was so tenuous that decomplexation to free BN-naphthalene **64** occurred at room temperature.

In their most recent report in this field, the Ashe group explored the ligand properties of deprotonated BN-styrene **65**, which was synthesized via the ring expansion route discussed above (Scheme 19).<sup>[61]</sup> The reaction of **65** with one equivalent of [Cp\*RuCl]<sub>4</sub> gave complex **66** in which BN-styrene is  $\eta^6$ -bound to ruthenium. However, when two equivalents of [Cp\*RuCl]<sub>4</sub> were added, diruthenium complex **67** was formed in which  $\eta^6$ -binding occurs between one ruthenium atom and the 1,2-azaborine ring, while the second ruthenium binds  $\eta^1$  to the 1,2-azaborine nitrogen and  $\eta^2$  to the *B*-vinyl group.

#### 4. The Liu Group – University of Oregon

Liu and coworkers have extended the synthetic methods developed by Ashe to create 1,2-azaborines with various heteroatom substituents at boron. Catalytic ring-closing metathesis in the presence of the reactive *B*-Cl bond of bisallyl aminoborane **46** readily furnished cyclized aminoborane **68** (Scheme 20).<sup>[62]</sup> Oxidation conditions were screened and it was determined that Pd black efficiently dehydrogenates **68** to give 1,2-azaborine **69**. Treatment with various carbon-based and heteroatomic nucleophiles provided the known 1,2-azaborine **49** as well as new 1,2-azaborine derivatives **70a–h** in good yield. Several of these derivatives are of particular interest as they relate to their phenyl analogs, including glycolate-substituted **70h**, which is isoelectronic with a known hypolipidemic agent.<sup>[63]</sup> The stability of 1,2-azaborines to H<sub>2</sub>O and O<sub>2</sub> was demonstrated for a series of boron- and C3-substituted derivatives and it was determined using kinetics experiments that substitution at these positions had a substantial effect on compound stability.<sup>[64]</sup>

In a subsequent report, Liu and coworkers demonstrated that the 1,2-azaborine analog of benzonitrile **71** was readily available by treating **69** with AgCN (Scheme 21).<sup>[65]</sup> The formation of the *B*-CN bond rather than the alternative *B*-NC bond was supported by calculations and was unambiguously confirmed by an isotopic labeling experiment using Ag<sup>13</sup>C<sup>15</sup>N. Complexation of **71** with chromium(0) led to a surprising isomerization of the CN group to form complex **72**, which was characterized by X-ray crystallography. Complex **72** was also readily available by the direct reaction of **69** with Na<sup>+</sup>[Cr(CO)<sub>5</sub>CN]<sup>-</sup>.

While the *B*-Cl bond in compound **69** is susceptible to nucleophilic aromatic substitution with a variety of anionic nucleophiles, less reactive neutral nucleophiles do not displace chloride from the boron atom. Liu and coworkers found that treatment of **69** with AgOTf smoothly forms species **73**, which contains the much more labile *B*-OTf bond. Compound **73** was shown to react with both electron-rich and electron-poor *para*-substituted pyridines to generate the first examples of 1,2-azaborine cations, **74a–e** (Scheme 22, top).<sup>[66]</sup> The solid-state fluorescence was measured for **74a–e** and compared to their all-carbon analogs. It was found that 1,2-azaborine substitution causes a red-shift of the emission maxima relative to the all-carbon species, and that the nature of the *para* substituent has a substantial effect on the emissive properties. Protonated pyridinium analogs of **74** (i.e., without the 1,2-azaborine group) were not fluorescent under identical conditions, confirming the critical role the 1,2-azaborine moiety plays in the observed emissions. In a later paper, the synthetic protocol was expanded to include substitution of **73** with trimethylphosphine,

triphenylphosphine oxide, and pyridine-*N*-oxide to generate the cationic 1,2-azaborines **75**–**77** (Scheme 22, bottom).<sup>[67]</sup>

The first successful synthesis of the parent 1,2-dihydro-1,2-azaborine **82** was reported by Liu and coworkers in 2009 (Scheme 23).<sup>[68]</sup> The incorporation of the *tert*-butyldimethylsilyl (TBS) nitrogen protecting group permitted the formation of a versatile 1,2-azaborine **78** via the same ring-closing/oxidation protocol presented above. Substitution at boron with superhydride provided *B*-H, *N*-TBS 1,2-azaborine **79**. Direct deprotection to the parent compound was unsuccessful, however treatment with (MeCN)<sub>3</sub>Cr(CO)<sub>3</sub> to form complex **80** activated the *N*-TBS group toward cleavage by HF-pyridine and afforded complex **81** in which 1,2-dihydro-1,2-azaborine is  $\eta^6$ -bound to the Cr(CO)<sub>3</sub> fragment. X-ray quality crystals of **81** were obtained, which showed that chromium is centered about the planar 1,2-dihydro-1,2-azaborine ring in analogy to the corresponding benzene-Cr(CO)<sub>3</sub> complex. Bond lengths, carbonyl-stretching frequencies, along with computationally predicted parameters are presented in Figure 5. Decomplexation of the 1,2-dihydro-1,2-azaborine ligand by exchange with PPh<sub>3</sub> provided **82** in good yield by <sup>1</sup>H NMR, however the volatility of **82** resulted in a low isolated yield. Compound **82** was characterized by <sup>1</sup>H, <sup>11</sup>B, and <sup>13</sup>C NMR spectroscopy, as well as IR spectroscopy and HRMS, which supported the assigned structure. The UV/vis spectrum of **82** is consistent with an aromatic heterocycle; the lowest energy absorption at 269 nm ( $\epsilon = 15632 \text{ M}^{-1}\text{cm}^{-1}$ ) is close in energy to the  $\alpha$  band of benzene (255 nm,  $\epsilon = 977 \text{ M}^{-1}\text{cm}^{-1}$ ), however this absorption was much stronger in **82**. The corresponding band in borazine is virtually non-existent. The electronic spectra indicate that **82** possesses significant aromatic character and more closely resembles benzene than borazine. 1,2-Dihydro-1,2-azaborine was found to be quite thermally and hydrolytically stable. Deuterium exchange at the *N*-H position occurred over approximately 24 hours in a CD<sub>3</sub>OD solution of **82**, demonstrating the unique reactivity of **82** relative to benzene.

The aromaticity of azaborine systems is of considerable interest not only from a fundamental point of view, but also as it relates to potential applications of BN/CC isosterism. Reactivity, structure, energy and magnetic criteria are the four metrics most used to characterize the aromaticity of a compound. Dewar, Ashe and others have demonstrated reactivity consistent with aromatic systems (e.g., electrophilic aromatic substitution,  $\pi$ -complexation), and the reported structures of azaborine compounds have indicated planarity and bond-lengths typical of aromatic systems. In a series of reports, the Liu group has endeavored to systematically characterize the aromaticity of 1,2-azaborine systems with regard to bond-delocalization, resonance stabilization energy, reactivity and magnetic properties. The results are summarized below.

Though the solid-state structural analysis of **82** (mp:  $-45 \text{ }^\circ\text{C}$ ) has not been reported, microwave spectroscopy has provided a means of elucidating the structural features. Kukolich, Liu, and coworkers recently collected microwave spectroscopic data for several isotopomers of **82**.<sup>[69]</sup> The results indicate that the 1,2-dihydro-1,2-azaborine ring is planar with a B–N bond length of 1.45(3) Å. The B–C and N–C bond lengths were found to be 1.51(1) Å and 1.37(3) Å, respectively. These bond lengths are somewhat longer than the values reported for substituted derivatives in the solid state (*vide infra*).

Liu and coworkers obtained evidence of bond delocalization in 1,2-azaborine via crystallographic analysis.<sup>[70]</sup> 1,2-azaborine precursor **83** was a versatile intermediate in the formation of a family of aminoboranes in various oxidation states with respect to the intraring carbon atoms (**84**–**87** in Scheme 24). Transition-metal catalysis was used in all cases to generate the desired heterocycle. The isomerization of **83** to B-vinyl **84** was achieved in good yield using Ru(Cl)<sub>2</sub>(PPh<sub>3</sub>)<sub>3</sub>. Alternatively, Ru(H)(Cl)(CO)(PPh<sub>3</sub>)<sub>3</sub> isomerized the olefin in **83** to N-vinyl **85**. Pd black catalyzed oxidation to 1,2-azaborine **86**. The same

catalyst in the presence of H<sub>2</sub> reduced **83** to **87**. Structural data for compounds **83–87** were obtained by single-crystal X-ray diffraction and are presented in Table 1. Upon oxidation to 1,2-azaborine **86**, the B–N bond lengthens relative to that in the other heterocycles. Similarly, the C=C bonds in **84** and **85** are shorter than the corresponding bonds in **86**. The lengthening of these formal double bonds in the structure of **86** is an indication of bond delocalization. Conversely, the C4–C5 single bond in **86** is shorter than the corresponding bonds in **84** and **85** by over 0.07 Å. A similar shortening of the B–C3 and C6–N bonds in 1,2-azaborine **86** versus all other derivatives is consistent with bond delocalization.

In 2010, Liu and coworkers reported the experimental determination of the resonance stabilization energy (RSE) of 1,2-azaborine, a quantitative measure of aromaticity.<sup>[71]</sup> By comparing the heat of hydrogenation (measured using reaction calorimetry) of the aromatic compound **89** against the sum of the heats of hydrogenation of the “pre-aromatic” compounds **90** and **91** [i.e.,  $RSE = \Delta H_1 - (\Delta H_2 + \Delta H_3)$ ], the RSE of 1,2-azaborine was found to be  $16.6 \pm 1.3$  kcal/mol, which is consistent with significant aromatic character (Scheme 25). This result is in good agreement with computationally predicted values for 1,2-azaborines, and quite a bit less than the RSE of benzene (32.4 kcal/mol).

Protons attached to aromatic systems typically display downfield NMR chemical shifts due to the shielding effects of the ring-current. Liu and coworkers have performed <sup>1</sup>H NMR experiments that confirm that azaborine protons are indeed shifted downfield as the molecules become aromatic. The NMR chemical shifts of the “pre-aromatic” compounds **90–92** along with the aromatic compound **89** are presented in Table 2. All protons were assigned using the 2D HETCOR technique. There is a clear down field shift ranging from 0.76 to 1.83 ppm as isolated olefinic protons become aromatic.

Complementing Ashe's pioneering work on electrophilic aromatic substitution of 1,2-azaborines, Liu and coworkers studied nucleophilic aromatic substitution of the parent 1,2-dihydro-1,2-azaborine **82**.<sup>[72]</sup> Treatment of **82** with two equivalents of nucleophile led to deprotonation at the nitrogen position and substitution at boron; reactions with only one equivalent of nucleophile had dramatically lower yields. Quenching with an appropriate electrophile (including  $\eta^+$ ) led to a diverse array of products, summarized in Table 3. Thorough experimental and computational mechanistic analysis revealed that the reaction most likely proceeds via two distinct pathways depending on the nature of the nucleophile.

In addition to exploring the fundamental properties of 1,2-azaborines, the Liu group is interested in utilizing these compounds in biological and materials science applications. A proof of concept demonstration of the biomimetic potential of 1,2-azaborine was reported in 2009 by Matthews, Liu, and coworkers.<sup>[73]</sup> The L99A mutant of T4 lysozyme is known to possess an internalized hydrophobic pocket that selectively binds aromatic hydrocarbons such as benzene. Using X-ray crystallography, neat 1,2-dihydro-1,2-azaborine **82** and *N*-ethyl 1,2-azaborine **70g** were found to diffuse into the hydrophobic pocket of crystalline L99A lysozyme in an identical manner to benzene and ethylbenzene, respectively. The selective binding of **82** within this hydrophobic pocket is quite interesting given the potential for the *N*-H group of **82** to undergo non-specific hydrogen bonding with the protein. Thus, 1,2-dihydro-1,2-azaborine effectively acts as a boron-containing hydrophobic benzene mimic in this specific pocket, and may provide access to the study of 1,2-azaborine in a biological context.

Indole is a ubiquitous heterocyclic motif in nature. It is found free in cells, as part of the amino acid tryptophan and the indole moiety is present in myriad natural products and biologically active compounds. Externally substituted, phenylenediamine-type BN-indole analogs were reported as early as 1957.<sup>[74]</sup> In 2010, Liu and coworkers reported the



syntheses and reactivity of the first internally substituted (“fused”) BN-indole derivatives.<sup>[75]</sup> The synthesis of *N*-*t*-Bu-protected BN-indole **93** is analogous to the route previously describe for monocyclic 1,2-azaborine derivatives (Scheme 26). It begins with the condensation of *N*-*t*-Bu-*N*-allylethylenediamine with *in situ* generated allylborondichloride to generate bisallyl species **94**. Ring-closing metathesis was found to proceed in high yield using Schrock's Mo RCM catalyst to give bicycle **95**. Both rings were dehydrogenated using Pd/C to give the desired product **93**. Electrophilic aromatic substitution (EAS) reactivity, which is a crucial reaction in the biochemistry of indoles (and one which has not been shown for externally BN substituted indole analogs), was demonstrated for **93**, and as with natural indole, EAS reactions of **93** were regioselective for the 3-position exclusively. EAS competition experiments between **93** and natural indole using dimethyliminium chloride revealed that **93** is significantly more nucleophilic.

In 2011, Liu and coworkers reported the synthesis of the parent “fused” BN-indole **96**.<sup>[76]</sup> This molecule contains the free *N*-H fragment that is an important feature in the biochemistry of indole and its derivatives. Synthesis was similar to the route described above, with a number of key distinctions (Scheme 27). First, the use of TBS rather than *t*-Bu as a nitrogen protecting group allowed for its facile removal later in the synthesis. Second, the use of Grubbs' first generation catalyst was found to be more effective for the RCM generation of **98** than Schrock's catalyst. Lastly, the use of perfluorodecalin as the solvent for the oxidation step allowed the aromatic product **99** to be recovered with simple THF extraction rather than distillation. The TBS group could be removed in the last step using *n*-Bu<sub>4</sub>NF to afford the product **96** in moderate yield. A non-disordered single crystal X-ray structure was obtained by cocrystallization of **96** with ethyl-4-chloro-3,5-nitrobenzoate and revealed **96** to be a planar molecule with bond-lengths consistent with aromatic delocalization. The optical and electronic properties of **96** were probed and compared to natural indole. BN-indole's absorption maximum is red-shifted from that of natural indole ( $\lambda = 293$  nm vs 268 nm in CH<sub>3</sub>CN). The emission maximum is likewise red-shifted for **96** compared to natural indole ( $\lambda_{em} = 360$  nm vs. 315 nm, in CH<sub>3</sub>CN) and displays a greater Stokes shift and lower quantum yield ( $\Phi = 0.08$  vs. 0.32 for indole). The red-shifted absorbance and emission maxima are consistent with a smaller HOMO-LUMO gap for **96**. Using <sup>1</sup>H NMR bracketing experiments, the pK<sub>a</sub> of the *N*-H proton was estimated to be ~30, which is roughly 9 orders of magnitude less acidic than natural indole (pK<sub>a</sub> = 20.95).

Boron-nitrogen containing compounds have received considerable attention as potential hydrogen storage materials due to their high hydrogen capacity and favorable kinetics of H<sub>2</sub> release. Moreover, calculations suggest that H<sub>2</sub> uptake and release by a combined CC/BN system should be essentially free energy-neutral (i.e.,  $\Delta G \approx 0$ ), potentially allowing efficient H<sub>2</sub> absorption/desorption with minimal energy input. Liu and coworkers have described a system by which 1,2-azaborines can potentially store and release three equivalents of H<sub>2</sub> per molecule (Scheme 28). As a proof of concept, they reported the mild regeneration of the “spent fuel” (i.e., aromatic, unsaturated) 1,2-azaborine to the “charged fuel” (i.e., fully H<sub>2</sub> saturated) amineborane fuel by the formal addition of three equivalents of H<sub>2</sub>.<sup>[77]</sup>

The first two equivalents of H<sub>2</sub> were added across the formal C=C bonds of **89** using catalytic hydrogenation with Pd/C and H<sub>2</sub> gas to give heterocycle **88** (Scheme 29). Under identical conditions, the reduction of benzene was not observed. The third equivalent of “H<sub>2</sub>” was added across the B-N bond in a sequential manner. The reaction of KH with **88** installed H<sup>-</sup> at the boron atom to give anionic intermediate **100**, which was then treated with HCl to give the fully charged fuel **101**.

As part of their effort to develop a BN-heterocycle based hydrogen storage platform, Liu and coworkers published an alternative route to fully saturated 6-membered BN-

heterocycles like **101**, including the parent 1,2-azaboracyclohexane **102** (Scheme 30).<sup>[78]</sup> Treatment of a bistrimethylsilyl-protected homoallylamine with  $\text{BH}_3 \cdot \text{THF}$  and subsequent addition of  $\text{KH}$  gave a monotrimethylsilyl-protected BN-cyclohexane potassium salt **103** in moderate yield. Deprotection/protonation with  $\text{HF} \cdot \text{pyridine}$  generated 1,2-azaboracyclohexane **102**. X-ray structural analysis confirmed the assigned structure, which, like cyclohexane, assumes a chair conformation. The free energy of activation for the chair flip was found to be significantly lower for **102** than for the all carbon version (8.8 vs 10.5 kcal/mol, under identical conditions), attributed to the longer B–N bond length (1.614(1) Å) vs. the C–C bond length in cyclohexane (1.51–1.53(1) Å) and to the shallow potential curve for the B–N stretch. Upon thermal activation (150 °C) **102** underwent a timerization reaction to form **104** with concomitant release of six equivalents of  $\text{H}_2$ . The conversion was clean and quantitative, in marked contrast to dehydrogenation reactions of ammonia borane ( $\text{H}_3\text{N}-\text{BH}_3$ ), which can produce various mixtures of oligomeric products depending on the dehydrogenation conditions used. Clean dehydrogenation to a well-defined single product using mild conditions make **102** a promising material for hydrogen storage. Additionally, the moderate hydrogen capacity of 4.7 wt.% can potentially be increased to 9.4 wt.% if the  $\text{H}_2$  release from BN can be coupled with dehydrogenation from the carbon positions as well.

In a further refinement of the intramolecular hydroboration/cyclization methodology described above, Liu and coworkers recently disclosed the synthesis of BN-methycyclopentane material **105** (Scheme 31).<sup>[79]</sup> This material is liquid at room temperature and can release hydrogen using cheap metal halide catalysts (e.g.,  $\text{FeCl}_2$ ) at 80 °C, both very desirable properties for potential hydrogen storage materials.

As part of their effort to develop  $\pi$ -conjugated azaborine optical materials, Liu and coworkers reported the synthesis and characterization of the BN analog of diphenylacetylene (tolan) (Scheme 32).<sup>[80]</sup> Synthesis of BN-tolan **107** and bis-BN-tolan **108** was achieved by reaction of the known TBS-protected precursor **78** with either phenylethynyl magnesium bromide or the Grignard reagent **109**. The resulting compounds were deprotected using a Cr-complexation route analogous to that used in the parent 1,2-dihydro-1,2-azaborine synthesis. Single crystal X-ray analysis revealed both compounds **107** and **108** to be linear with respect to the B–C $\equiv$ C–X axis with a coplanar orientation of the aromatic rings, which is indicative of significant  $\pi$ -overlap throughout the bicycle. The other noteworthy feature of the crystal structure was the observation dimers formed through a rarely seen N–H– $\pi$ (C $\equiv$ C) hydrogen bonding interaction. UV/vis absorbance maxima for **107** and **108** are centered at 299 nm and are broadened relative to tolan. Emission maxima in THF for **107** and **108** are 350 nm ( $\Phi = 0.012$ ) and 388 nm ( $\Phi = 0.020$ ), respectively, which are significantly red-shifted from tolan (317 nm,  $\Phi = 0.007$ ); the emissions display minimal solvatochromism.

One of the most exciting recent developments to emerge from the Liu group is the disclosure of the first example of a 1,3-azaborine.<sup>[81]</sup> This significant synthetic achievement was accomplished by harnessing the power of ring-closing metathesis and tin chemistry previously developed in the Liu group, with several substantial modifications (Scheme 33). The stannane reagent **110** was produced in two steps from allylmethylamine, formaldehyde and benzotriazole. Direct transmetalation between **110** and the vinylboron chloride **111** was unsuccessful, however lithium-tin exchange followed by addition of the electrophile **111** afforded the RCM precursor **112** in modest yield. Both Grubbs' first generation and Schrock's catalysts failed to cyclize **112**, presumably due to degradation of the catalyst caused by the relatively nucleophilic amine. This was overcome by first forming the ammonium salt of **112** with triflic acid, closing the ring using Grubbs' first generation catalyst, and finally deprotonating the ring-closed ammonium salt with DBU to furnish **113**.

Dehydrogenation of **113** to generate the aromatic final product also proved to be a challenge, with significant formation of fully reduced species **114** (2.2:1 **114/115**) observed even under optimized conditions. The desired product was isolated by distillation and fully characterized. Single crystal X-ray analysis revealed that the 1,3-azaborine ring is completely planar, with intra-ring bond-lengths consistent with electron delocalization. To further probe the aromatic nature of the 1,3-azaborine ring, **114** was treated with  $(\text{MeCN})_3\text{Cr}(\text{CO})_3$  to generate the piano-stool complex. A close inspection of the crystal structure of the complex showed that it is best characterized as an  $\eta^5 \pi$ -complex in which the boron atom does not participate, as it lies 0.21 Å above the root-mean-square of the plane containing the other five atoms. Compound **114** was found to be inert to a variety of nucleophiles, but reacts with acetic acid to form a *B*-OAc adduct. Electrophilic aromatic substitution reactivity was also probed, and **114** was found to undergo EAS regioselectively in the presence of dimethyl(methylene)ammonium chloride.

## 5. The Perepichka Group – McGill University

In 2010 Perepichka and coworkers investigated the incorporation of 1,2-azaborines into oligothiophene organic electronic materials.<sup>[82]</sup> Structurally related thienoazaborine and dithienoazaborines have been reported, but their optoelectronic properties were not explored in depth. The addition of boron into conjugated systems has been shown to increase luminescence efficiency and improve light-emitting properties of a material.<sup>[83]</sup> The Lewis acidic boron centers have typically been stabilized through steric screening using bulky aryl substituents, but in the solid state these groups can suppress  $\pi$ -stacking critical to intermolecular charge transfer. In 1,2-azaborines the boron center is stabilized through orbital interactions with a lone pair of electrons from the adjacent nitrogen atom and the resulting planar molecules should not interfere with  $\pi$ -stacking.

Treatment of known diaminothiophene **116** with excess  $\text{PhBCl}_2$  (a synthetic strategy reminiscent of Dewar's early work) afforded bis-azaborine **117** (Scheme 34). It was anticipated that the strong acidity of the *N*-H protons could be problematic for the intended applications or further functionalization, so the ethylene-linked species **120** was synthesized by borylation of the ethylenediaminothiophene compound **119**. The ethylene linker does not distort the planarity of the ring system. X-ray crystallographic analysis of **117** and **120** revealed B–N bond lengths of 1.405–1.460 Å, similar to other reported azaborines and consistent with electron delocalization in the azaborine ring. The structures were almost planar with regard to thiophene rings, however the phenyl rings lie out of the plane, limiting their conjugation with the polycyclic moiety. Both compounds formed slipped  $\pi$ -stacks with alternating head-to-tail orientation and interplanar distances between the parallel thiophene ring systems of 3.47–3.83 Å.

Analysis of UV/vis absorption spectra for **117** and **120** revealed that the ethylene bridge does not significantly affect the electronic structure; both compounds display almost identical absorption spectra ( $\lambda_{\text{abs}} = 395$  and  $397$  for **117** and **120**, respectively).  $\lambda_{\text{max}}$  for **117** and **120** is red-shifted compared to non-fused terthiophene (354 nm) and S-bridged pentathienoacene (357 nm). Compounds **117** and **120** exhibit deep-blue photoluminescence at  $\lambda_{\text{max}} = 407$ – $410$  nm, with  $\Phi_{\text{PL}} = 25$ – $34\%$ . Redox properties for the two compounds were studied by cyclic voltammetry. Both compounds undergo irreversible electrochemical oxidation with anodic peak potential  $E_{\text{pa}}$  at 0.48 V vs  $\text{Fc}/\text{Fc}^+$ , ca. 0.2 V more positive than diaminoterthiophene and consistent with the electron withdrawing effects of boron.

The stabilizing effect of the intramolecular Lewis acid-base interaction between nitrogen and boron was probed by introducing weak to moderate Lewis bases to solutions of **117** and **120**. No complexation was detected with  $\text{H}_2\text{O}$ , THF, amines,  $\text{Cl}^-$ ,  $\text{Br}^-$ ,  $\text{I}^-$ ,  $\text{OH}^-$ , or  $\text{OCH}_3^-$ .

However, addition of  $\text{Bu}_4\text{NF}$  to solutions of **120** led to the formation of a mono-fluoride adduct, even in the presence of a very large excess of  $\text{F}^-$ . The binding constant ( $\log K_a = 3.3 \pm 0.1$  in  $\text{CH}_2\text{Cl}_2$ ) is lower than that of triarylboranes without electronic stabilization of the empty p-orbital (e.g.,  $\log K_a = 6.3$  for dithienylmesitylborane in  $\text{CH}_2\text{Cl}_2$ ). The emission band of the fluoride adduct is red-shifted to 540 nm with a corresponding color change from blue to green observable by the naked eye. While fluoride sensing by conjugated boron derivatives is well known, most systems are characterized by a blue-shift of the absorbance and quenching of the fluorescence. The authors propose that systems based on **120** could be used as an “off-on” sensor for  $\text{F}^-$ .

In a subsequent report, Perepichka and coworkers subjected the compounds **117** and **120** to higher oxidation potentials and discovered interesting electropolymerization reactivity that ultimately led to the expulsion of boron and the formation of a low band-gap polymer.<sup>[84]</sup> Through careful isolation of partially deborylated donor-acceptor oligomer intermediates **121** and **122** and comprehensive spectroscopic characterization, they were able to elucidate the composition of the insoluble polymer **123**. The proposed formation of electrochemical products is illustrated in Scheme 35.

Controlled potential electrolysis of solutions of **117** was performed at 100 mV more positive than the first oxidation wave. During the first oxidation process, boron elimination and the formation of a new C–C bond between the thiophene and phenyl ring occurs to give species **121**. The first oxidation process of **121** does not lead to boron elimination but instead to a radical coupling process to form the dimer **122** (as in usual thiophene polymerization). Exposing **122** to high potential (1.07 vs  $\text{FC}/\text{FC}^+$ ) led to the formation of polymer films analogous to those grown directly from **117**.

The optical properties of **121** and **122** were probed by UV/vis and fluorescence spectroscopy. **121** displays blue-shifted absorption ( $\lambda_{\text{max}} = 352$  nm,  $\log \epsilon = 4.1$ ) compared to the starting material **117** ( $\lambda_{\text{max}} = 391$  nm), attributed to an out-of-plane shift of the deborylated thiophene ring. **122** has a red-shifted absorption compared to both **117** and **121** ( $\lambda_{\text{max}} = 420$  nm,  $\log \epsilon = 4.0$ ) due to extended  $\pi$ -conjugation. The fluorescence spectra of **121** and **122** exhibit large Stokes shifts of 0.9 and 0.6 eV ( $6950$  and  $5013$   $\text{cm}^{-1}$ ), respectively, which points to large structural rearrangements in the excited state. The emission color shifts from deep-blue for **117** to sky-blue for **121** to bright-green-yellow for the dimer **122**.

## 6. The Yamaguchi Group – Nagoya University

Yamaguchi and coworkers recently reported the synthesis of 1,2-azaborine in an extended  $\pi$ -conjugated system, unexpectedly obtained in the course of their studies of triarylborane-based functional materials.<sup>[85]</sup> Attempts to remove the Boc protecting group from triarylborane species **124** by treatment with  $\text{BF}_3 \cdot \text{OEt}_2$  in refluxing THF led to a complex mixture of products (Scheme 36). Careful separation using preparative gel permeation chromatography enabled the isolation of migratory ring expanded product **125** in 13% yield along with products (totalling 60% yield) resulting from the cleavage of the pyrrole-boron bond. Seizing the opportunity to investigate the potential utility of 1,2-azaborine as a building block in  $\pi$ -conjugated materials, structural, photophysical and electrochemical studies of **125** were undertaken and the results were compared with the all carbon analog **126**.

Two crystallographically independent molecules of **125** exist in a unit, with reasonably coplanar  $\pi$ -conjugated skeletons. Dihedral angles between the pyrrole and the azaborine and between the azaborine and the phenyl group are in the range of  $7\text{--}14^\circ$  and  $30\text{--}34^\circ$ ,

respectively. The bulky Tip (2,4,6-triisopropylphenyl) group does not impede  $\pi$ -conjugation over the framework, but prevents intermolecular  $\pi$ - $\pi$  interactions. Analysis of bond lengths in the azaborine portion of **125** revealed that the B–N moiety has less double bond character than an isolated B–N bond due to  $\pi$ -conjugation in the azaborine ring, however the extension of the  $\pi$ -conjugation at the 3 and 6 positions may decrease the aromatic character of the azaborine ring compared to non- $\pi$ -extended 1,2-azaborines.

In  $\text{CH}_2\text{Cl}_2$ , UV/vis absorbance and fluorescence maxima for **125** are red-shifted from the all-carbon analog **126** by 57 and 70 nm, respectively. Both compounds show only subtle solvatochromism in both the absorbance and emission spectra. **125** has very high quantum yields, close to unity even in polar solvents like MeOH and significantly higher than **126**.

Cyclic voltammetry experiments performed on **125** and **126** indicate a higher HOMO level and a narrower HOMO-LUMO gap for **125**, consistent with the red-shifted absorption maximum. The authors reasoned that the differences in the redox potential and photophysical properties between **125** and **126** are due to the *nonaromatic* character of the azaborine ring. In this context, the azaborine ring can be considered a cyclic butadiene analog and, in fact, DFT calculations at the B3LYP/6-31G(d) level revealed that the frontier orbital energy levels of **125** are more similar to a cyclohexa-1,3-diene model than the benzene-containing **126**. NICS(0) calculations performed on the 1,2-azaborine ring in **125** were slightly more positive (–4.73 ppm) than the parent 1,2-azaborine (–5.10 ppm), indicative of decreased aromaticity.

## 7. The Kawashima Group – University of Tokyo

Kawashima and coworkers have explored the incorporation of the 1,4-azaborine motif into anthracene and ladder-type pentacene and heptacene analogs, with the goal of utilizing these compounds in OLED devices.<sup>[86]</sup> The synthesis of BN-pentacene **128** was achieved by treatment of the para-diamino arene **127** with  $\text{MesB}(\text{OMe})_2$  (Scheme 37). Similar transformations from meta-diamino arene **129** and triaminoarene **131** generated **130** and **132**, respectively. All three compounds were air- and moisture-stable, which was ascribed in part to the sterically demanding mesityl substituents at boron.

The X-ray crystal structure of **128** revealed that the BN-pentacene framework is virtually coplanar, indicating an extended  $\pi$ -conjugated system. No evidence of intermolecular  $\pi$ -stacking was observed due to the bulky mesityl groups, which interfere with close packing. The absorption and emission properties of **128**, **130** and **132** were examined and are summarized in Table 4. The absorption and emission maxima observed for **128** and **132** are red-shifted relative to BN-anthracene, which is consistent with extended conjugation. On the other hand, BN-pentacene **130**, in which the 1,4-azaborine rings are oriented parallel to each other, displayed optoelectronic properties which were very similar to BN-anthracene.

After their initial report on BN-pentacene and heptacene analogs, Kawashima and coworkers developed a more general route to substituted 1,4-azaborine containing anthracene as well as previously described anti-parallel pentacene derivatives (Scheme 38).<sup>[87]</sup> An ortho-selective dilithiation of **133** and subsequent treatment with arylboronic esters generated dibromo-substituted products **134**, which could be further elaborated via Buchwald-Hartwig amination, Sonogashira cross-coupling or lithium-halogen exchange/electrophile addition (MeI) to give products **135–137**. The same protocol could be expanded to the synthesis of ladder-type azaborines via tetralithiation of **138**. The brominated product of this reaction, compound **139** could not be isolated due to poor solubility, however solubilizing groups could be added to the crude mixture and the substituted BN-pentacene compounds **140a–c** could be isolated in moderate yield.



UV/vis spectra for compounds bearing electron-donating amino groups (i.e., HexNH in **135a** and Ph<sub>2</sub>N in **135b**) showed red-shifted absorptions relative to the reference compound, Me-substituted **137a**, due to elevation of the HOMO level. The carbazolyl-substituted BN-anthracene **135c** had an absorption wavelength close to the reference compound and had a fluorescence quantum yield of unity, attributed to molecular rigidity. The ladder-type azaborines **140a–c** displayed similar absorbance properties, with red-shifted absorption maxima corresponding to increasing electron donating ability of the pendant amine groups. The carbazolyl substituted derivative **140c** also showed the highest fluorescence quantum yield.

In a subsequent report, Kawashima and coworkers utilized the same general reaction sequence to develop dicationic ammonium and phosphonium functionalized BN-acenes **141** and **142**, capable of acting as fluorescent sensors for biologically relevant anions such as fluoride and cyanide (Scheme 39).<sup>[88]</sup> These compounds retain the optical properties of the azaborine motif and do not aggregate in aqueous media. The complexation ability of ammonium functionalized species **141** with all anions screened was too weak to observe via UV/vis or fluorescence spectroscopy, however the phosphonium species **142** displayed a very high affinity for the cyanide ion and was almost inactive against other environmentally common anions under the testing conditions. Titration experiments were used to find the complex formation constant between **142** and the cyanide ion ( $1.2(4) \times 10^5 \text{ M}^{-1}$  in DMSO/H<sub>2</sub>O (4:6 v/v) and  $5.2(5) \times 10^4 \text{ M}^{-1}$  in 100% H<sub>2</sub>O). Fluorescence quenching experiments with various anions revealed that only CN<sup>-</sup> quenched the emission of **142** to a degree that was clearly observable with the naked eye.

Around the same time, Kawashima and coworkers reported the synthesis and fluoride sensing ability of a bis(dimesitylboryl)azaborine **143**, again taking advantage of the general synthetic methodology they had previously developed (Scheme 40, series a).<sup>[89]</sup> Their rationale for the introduction of strong  $\pi$ -acceptors (i.e., Mes<sub>2</sub>B) into the 1,4-azaborine framework was two-fold: First, the Mes<sub>2</sub>B group decreases the LUMO energy level, thus increasing the Lewis acidity of the azaborine unit. Second, coordination of multiple Lewis bases to the peripheral boron atoms (in addition to the azaborine boron center) can alter the donor-acceptor interactions within the molecule and thus vary the absorption and emission color based on the amount of guest ion. The introduction of dimesitylboryl groups resulted in a hypsochromic shift in the absorbance maximum (377 nm vs. 405 nm for the *N*-Me derivative of **137a**) and a ~10 fold increase in the extinction coefficient. To investigate the Lewis base detection ability, **143** was treated with excess (*n*-Bu)<sub>4</sub>NF and monitored via FAB mass spectrometry and <sup>11</sup>B NMR. Signals consistent with the formation of **144a** and **145a**, rather than **146a** were observed (i.e., shifting of the peak corresponding to Mes<sub>2</sub>B groups but not the azaborine peak). This conclusion was supported by molecular orbital calculations, which show that the LUMO is distributed over the two Mes<sub>2</sub>B groups, kinetically favoring Lewis base coordination at those sites. UV/vis titration of **143** with (*n*-Bu)<sub>4</sub>NF showed the stepwise formation of **144a** and **145a** and the values of K<sub>1</sub> and K<sub>2</sub> were determined to be  $>10^8 \text{ M}^{-1}$  and  $7 \times 10^5 \text{ M}^{-1}$ , respectively. Fluorescence spectrometry could also be used to monitor complex formation and it was possible to detect the fluoride ion at sub-micromolar concentrations. However, because of the much smaller value of K<sub>2</sub> than K<sub>1</sub>, the blue-shifted emission band corresponding to species **145a** was only visible upon addition of a large excess of fluoride ion.

In another report published in 2009, Kawashima and coworkers used the bis(dimesitylboryl)azaborine **143** for multistep detection of the cyanide ion (Scheme 40, series b).<sup>[90]</sup> In the case of CN<sup>-</sup>, the values of both K<sub>1</sub> and K<sub>2</sub> exceed the limit of precise estimation ( $>10^8 \text{ M}^{-1}$  in THF), thus the cyanide ion seems to form a much stronger complex with **143** than the fluoride ion does, despite boron's affinity for fluoride. The fluorescent

color shift from violet ( $\lambda=420$  nm) corresponding to the monocyanoborate species **144b** to blue ( $\lambda=433$  nm) corresponding to dicyanoborate **145b** was visible with the naked eye upon addition of just 2.6 equiv. of  $\text{CN}^-$ .

The Kawashima group has also reported the construction of  $\pi$ -conjugated dendrimeric structures based on a 1,4-BN-anthracene branching unit featuring additional pendant BN-acene groups (Scheme 41).<sup>[91]</sup> Conjugated dendrimers bearing both electron donors and acceptors are expected to show n-type or ambipolar charge transfer ability, both of which are important in organic field effect transistors. Both the branching and terminal BN-acene moieties were synthesized in a similar manner to the compounds described above, and the dendron arms were synthesized by Pd-catalyzed coupling reactions between branching and terminal units. The optical properties of the dendrons are similar to those of the parent azaborines, indicating that the azaborine units are aligned perpendicularly to each other. Dendrimers **147–149** were constructed from TMS protected dendrons using standard Sonogashira conditions. Emission from the dendrimers stems from an intramolecular charge transfer (ICT) between the dendrons and the core. DFT calculations suggest that electron transfer from the dendrons to the core is thermodynamically favorable process, but experimental results indicate that the fate of the ICT excited states strongly depends on the generation of the dendron.

In 2010 Kawashima and coworkers reported the synthesis of a dinaphthoazaborine based on a modification of their general synthetic methodology (Scheme 42).<sup>[92]</sup> Dilithiation of the dibromoamino species **150** with subsequent addition  $\text{MesB(OMe)}_2$  at  $-78$  °C afforded the dinaphthoazaborine **151**. Analysis of the single crystal X-ray structure of **151** showed that the dinaphthoazaborine skeleton is butterfly-like and the angle between the two naphthalene rings is  $15^\circ$ , compared to the  $9^\circ$  (average) bent angle between the two benzene rings of the *N*-Me derivative of **137a**. In contrast to **137a**, there are clear intermolecular  $\pi$ - $\pi$  and CH- $\pi$  interactions between molecules of **151** in the solid state, which affect its solid-state fluorescence properties. In hexanes, the UV/vis absorbance maximum for **151** ( $\lambda = 519$  nm) is red-shifted by 114 nm from that of **137a**, indicating elongation of the  $\pi$ -system and a decreased HOMO-LUMO energy gap. Emission maximum of **151** is red-shifted by 103 nm, however the quantum yield is lower than that of **137a**. Also, unlike **137a**, **151** does not show detectable solid-state fluorescence. Electrochemical analyses revealed that **151** forms a stable radical anion at relatively low potential ( $-2.1$  V vs.  $\text{Cp}_2\text{Fe/Cp}_2\text{Fe}^+$ ), which could lead to possible applications as an electron-acceptor and anion sensor.

## 8. The Nakamura Group – Kyoto University

Hatakeyama, Nakamura and coworkers very recently reported an efficient route to BN-fused analogs of polycyclic aromatic hydrocarbons (PAHs), based on a tandem intramolecular electrophilic arene borylation protocol (Scheme 43).<sup>[93]</sup> Facile access to this structural motif allowed them to characterize these materials with an eye toward potential applications in organic electronic functional materials. The arene borylation precursor, dichloroboraneamine **153** was generated *in situ* from bis(biphenyl-2-yl)amine **152**. After screening a variety of Lewis acids and Brønsted bases, it was found that treatment of **153** with 4 equivalents of  $\text{AlCl}_3$  and 1.5 equivalents of 2,2,6,6-tetramethylpiperidene (TMP) afforded the BN-PAH **154** in 67% yield. It was also determined that the  $\text{AlCl}_3$ /TMP stoichiometry is critical to achieving a high yield. The same optimized conditions could be used to generate the bis-BN-fused PAH **156** from starting amine **155**.

The X-ray crystal structure of **154** revealed that the B-N bond-length (1.426(3) Å) is shorter than typical BN-aromatics (1.45–1.47 Å) and more consistent with a B=N double bond. B-C and N-C bond-lengths are consistent with single bond character. The low apparent

aromaticity of the azaborine ring is in agreement with the calculated NICS(1) value of  $-2.9$ . In the solid state, **154** adopts a twisted configuration at the heteroatom bridge and an alternating enantiomeric (i.e., left- or right-handed) helical packing structure. The all-carbon analog of **154**, dibenzo[*g,p*]chrysene, was also analyzed by X-ray crystallography and displayed remarkably similar solid state parameters (e.g., twisted structure with significant double bond character of bridging C–C bond) and similar physical properties, including melting point ( $229\text{ }^{\circ}\text{C}$  vs.  $227\text{ }^{\circ}\text{C}$  for **154**). However, the solubility of **154** was much higher than dibenzo[*g,p*]chrysene in common organic solvents, presumably due to its dipole moment. Surprisingly, despite its extended polycyclic aromatic structure, **156** was found to be moderately soluble in organic solvents such as chloro- and 1,2-dichlorobenzene.

Using time-resolved microwave conductivity measurements, **154** was found to have high intrinsic hole mobility ( $0.07\text{ cm}^2\text{ V}^{-1}\text{ s}^{-1}$ ), ten times higher than dibenzo[*g,p*]chrysene, and rivalling rubrene ( $0.05\text{ cm}^2\text{ V}^{-1}\text{ s}^{-1}$ ), one of the most popular organic semiconductors. The superior hole mobility of **154** was attributed to partial localization of the frontier orbitals induced by BN-substitution, which strengthens the electronic coupling between neighboring atoms in the solid state. The favorable electronic properties, straightforward synthesis and surprising solubility make **154** and **156** suitable for use in organic electronics.

## 9. Emerging Applications and Future Directions

From the breadth of synthetic approaches and novel reactivity presented here it is clear that the ubiquity of the arene motif coupled with the unique properties stemming from BN/CC isosterism present no shortage of potential applications for this chemistry. BN incorporation into aromatic scaffolds can lend favorable properties to organic optoelectronic materials, and create highly selective molecular ion sensing platforms. The dual hydridic/protic nature of B–H/N–H bonds can be harnessed for chemical hydrogen storage. BN/CC isosterism can also be used as a way to “disguise” boron for potential biological applications. The study of BN-aromatic compounds can also enrich our fundamental understanding of aromaticity itself. Emerging synthetic techniques stemming from this research may further expand the toolkit available to curious chemists in other fields as well.

## Biographies



Patrick G. Campbell was born in Juba, South Sudan in 1982, and grew up in the damp yet scenic hills of Seattle, WA, USA. He received his BA in Chemistry from Macalester College in St. Paul, MN in 2005. He is currently a Ph.D. candidate at the University of Oregon. His research interests include the application of CBN heterocycles as hydrogen storage materials and as arene mimics in novel phosphine-centered ligands for transition-metal catalysis.



Dr. Adam J. V. Marwitz was born in Laramie, WY, in 1981 and received his B. S. degree in Chemical Engineering from the Colorado School of Mines in 2004. In 2010, he completed his Ph.D. at the University of Oregon under the direction of Professor Shih-Yuan Liu, investigating the chemistry of the 1,2-dihydro-1,2-azaborine heterocycle. He is currently a post-doctoral fellow at the University of Calgary under the supervision of Professor Warren Piers.



Prof. Shih-Yuan Liu was born in Hsinchu, Taiwan in 1975. His family moved to Austria when he was ten. He began his undergraduate studies in Chemistry at Vienna University of Technology in 1994. In 1998 he received his first diploma (B.S. equivalent) from Vienna University of Technology. He did his doctoral work at MIT with Prof. Gregory C. Fu and received his Ph.D. degree in organic chemistry in 2003. He then pursued his postdoctoral studies in inorganic chemistry with Prof. Daniel G. Nocera, also at MIT. Prof. Shih-Yuan Liu began his independent career at the University of Oregon in 2006, where he is currently an Assistant Professor of Chemistry.

## References

- [1]. Lipscomb WN. *Angew. Chem.* 1977; 89:685–696.
- [2]. Brown HC. *Angew. Chem.* 1980; 92:675–683.
- [3]. Suzuki A. *Angew. Chem. Int. Ed.* 2011; 50:6722–6737.
- [4]. Burkhardt ER, Matos K. *Chem. Rev.* 2006; 106:2617–2650. [PubMed: 16836295]
- [5]. Miyaura N, Suzuki A. *Chem. Rev.* 1995; 95:2457–2483.
- [6]. Suginome M. *J. Synth. Org. Chem., Jpn.* 2007; 65:1048–1059.
- [7]. Yamashita M. *Angew. Chem. Int. Ed.* 2010; 49:2474–2475.
- [8]. Baker SJ, Tomsho JW, Benkovic SJ. *Chem. Soc. Rev.* 2011; 40:4279–4285. [PubMed: 21298158]
- [9]. Hudson ZM, Wang S. *Dalton Trans.* 2011; 40:7805–7816. [PubMed: 21603687]
- [10]. Pritchard RH, Kern CW. *J. Am. Chem. Soc.* 1969; 91:1631–1635.
- [11]. Blanksby SJ, Ellison GB. *Acc. Chem. Res.* 2003; 36:255–263. [PubMed: 12693923]
- [12]. Thorne LR, Suenram RD, Lovas FJ. *J. Chem. Phys.* 1983; 78:167.
- [13]. Grant DJ, Dixon DA. *J. Phys. Chem. A.* 2006; 110:12955–12962. [PubMed: 17125312]
- [14]. Alkorta I, Elguero J. *Struct. Chem.* 1998; 9:59–63.
- [15]. Sugie M, Takeo H, Matsumura C. *Chem. Phys. Lett.* 1979; 64:573–575.

- [16]. Green IG, Johnson KM, Roberts BP. *J. Chem. Soc., Perkin Trans. 2.* 1989:1963–1972.
- [17]. Stock A, Pohland E. *Ber. Dtsch. Chem. Ges.* 1926; 59:2210–2215.
- [18]. For pioneering contributions by Wiberg in borazine chemistry, see: Wiberg E, Bolz A. *Ber. Dtsch. Chem. Ges.* 1940; 73:209–232.. Wiberg E, Hertwig K, Bolz A. *Z. Anorg. Allg. Chem.* 1948; 256:177–252.. Wiberg E, Hertwig K. *Z. Anorg. Allg. Chem.* 1948; 257:138–144.
- [19]. Li J-S, Zhang C-R, Bin Li, Cao F, Wang S-Q. *Inorg. Chim. Acta.* 2011; 366:173–176.
- [20]. Lisovenko AS, Timoshkin AY. *Inorg. Chem.* 2010; 49:10357–10369. [PubMed: 20964381]
- [21]. Braunschweig H, Green H, Radacki K, Uttinger K. *Dalton Trans.* 2008:3531–3534. [PubMed: 18594698]
- [22]. Kesharwani MK, Suresh M, Das A, Ganguly B. *Tetrahedron. Lett.* 2011; 52:3636–3639.
- [23]. Yamamoto Y, Miyamoto K, Umeda J, Nakatani Y, Yamamoto T, Miyaura N. *J. Organomet. Chem.* 2006; 691:4909–4917.
- [24]. Islas R, Chamorro E, Robles J, Heine T, Santos JC, Merino G. *Struct. Chem.* 2007; 18:833–839.
- [25]. Bean DE, Fowler PW. *J. Phys. Chem. A.* 2011; 115:13649–13656. [PubMed: 21954962]
- [26]. Soncini A, Domene C, Engelberts JJ, Fowler PW, Rassat A, van Lenthe JH, Havenith RWA, Jenneskens LW. *Chem. -Eur. J.* 2005; 11:1257–1266. [PubMed: 15627952]
- [27]. Phukan AK, Guha AK, Silvi B. *Dalton Trans.* 2010; 39:4126–4137. [PubMed: 20390175]
- [28]. Bosdet MJD, Piers WE. *Can. J. Chem.* 2009; 87:8–29.
- [29]. Ulrich G, Ziesel R, Harriman A. *Angew. Chem. Int. Ed.* 2008; 47:1184–1201.
- [30]. Claessens CG, González-Rodríguez D, Torres T. *Chem. Rev.* 2002; 102:835–853. [PubMed: 11890759]
- [31]. Dewar MJS, Kubba VP, Pettit R. *J. Chem. Soc.* 1958:3073–3076.
- [32]. Dewar MJS. *Tetrahedron.* 1959; 7:213–222.
- [33]. Dewar MJS, Kubba VP. *J. Org. Chem.* 1960; 25:1722–1724.
- [34]. Dewar MJS, Kubba VP. *J. Am. Chem. Soc.* 1961; 83:1757–1760.
- [35]. Dewar MJS, Maitlis PM. *J. Am. Chem. Soc.* 1961; 83:187–193.
- [36]. Dewar MJS. *Tetrahedron.* 1961; 15:35–45.
- [37]. Dewar MJS, Dietz R. *J. Chem. Soc.* 1959:2728.
- [38]. Dewar MJS, Dietz R, Kubba VP, Lepley AR. *J. Am. Chem. Soc.* 1961; 83:1754–1756.
- [39]. Dewar MJS. *Tetrahedron.* 1961; 15:26–34.
- [40]. Dewar MJS, Dietz R. *J. Org. Chem.* 1961; 26:3253–3256.
- [41]. Dewar MJS, Hashmall J, Kubba VP. *J. Org. Chem.* 1964; 29:1755–1757.
- [42]. Dewar MJS, Gleicher GJ, Robinson BP. *J. Am. Chem. Soc.* 1964; 86:5698–5699.
- [43]. Dewar MJS, Jones R. *Tet. Lett.* 1968; 22:2707–2708.
- [44]. Dewar MJS, Marr PA. *J. Am. Chem. Soc.* 1962; 84:3782.
- [45]. White DG. *J. Am. Chem. Soc.* 1963; 85:3634–3636.
- [46]. Davies KM, Dewar MJS, Rona P. *J. Am. Chem. Soc.* 1967; 89:6294–6297.
- [47]. Ferles M, Polivka Z. *Collect. Czech. Chem. Commun.* 1968; 33:2121–2129.
- [48]. Polivka Z, Kubelka V, Holubova N, Ferles M. *Collect. Czech. Chem. Commun.* 1970; 35:1131–1146.
- [49]. Wille H, Goubeau J. *Chem. Ber.* 1972; 105:2156–2168.
- [50]. Wille H, Goubeau J. *Chem. Ber.* 1974; 107:110–116.
- [51]. Gronowitz S, Ander I. *Chemica Scripta.* 1980; 15:23–26.
- [52]. Gronowitz S, Ander I. *Chemica Scripta.* 1980; 15:135–144.
- [53]. Gronowitz S, Ander I. *Chemica Scripta.* 1980; 15:145–151.
- [54]. Ashe AJ, Fang. *Org. Lett.* 2000; 2:2089–2091. [PubMed: 10891237]
- [55]. Ashe AJ, Fang X, Fang X, Kampf J. *Organometallics.* 2001; 20:5413–5418.
- [56]. Pan J, Kampf JW, Ashe AJ. *Organometallics.* 2004; 23:5626–5629.
- [57]. Pan J, Kampf JW, Ashe AJ. *Organometallics.* 2008; 27:1345–1347.
- [58]. Fang X, Yang H, Kampf J, Holl M, Ashe AJ. *Organometallics.* 2006; 25:513–518.



- [59]. Pan J, Kampf JW, Ashe AJ. *Org. Lett.* 2007; 9:679–681. [PubMed: 17249680]
- [60]. Pan J, Kampf JW, Ashe AJ. *Organometallics.* 2009; 28:506–511.
- [61]. Pan J, Kampf JW, Ashe AJ. *J. Organomet. Chem.* 2009; 694:1036–1040.
- [62]. Marwitz AJV, Abbey ER, Jenkins JT, Zakharov LN, Liu S-Y. *Org. Lett.* 2007; 9:4905–4908. [PubMed: 17944483]
- [63]. Zúñiga C, Garduño L, del Carmen Cruz MA, Salazar MA, Pérez-Pastén R, Chamorro GN, Labarrios F, Tamariz JN. *Drug Dev. Res.* 2005; 64:28–40.
- [64]. Lamm AN, Liu S-Y. *Mol. Biosyst.* 2009; 5:1303–1305. [PubMed: 19823745]
- [65]. Marwitz AJV, McClintock SP, Zakharov LN, Liu S-Y. *Chem. Commun.* 2010; 46:779–781.
- [66]. Marwitz AJV, Jenkins JT, Zakharov LN, Liu S-Y. *Angew. Chem. Int. Ed.* 2010; 49:7444–7447.
- [67]. Marwitz AJV, Jenkins JT, Zakharov LN, Liu S-Y. *Organometallics.* 2011; 30:52–54. [PubMed: 21278846]
- [68]. Marwitz AJV, Matus MH, Zakharov LN, Dixon DA, Liu S-Y. *Angew. Chem. Int. Ed.* 2009; 48:973–977.
- [69]. Tanjaro C, Daly A, Marwitz AJV, Liu S-Y, Kukolich S. *J. Chem. Phys.* 2009; 131:224312. [PubMed: 20001041]
- [70]. Abbey ER, Zakharov LN, Liu S-Y. *J. Am. Chem. Soc.* 2008; 130:7250–7252. [PubMed: 18479099]
- [71]. Campbell PG, Abbey ER, Neiner D, Grant DJ, Dixon DA, Liu S-Y. *J. Am. Chem. Soc.* 2010; 132:18048–18050. [PubMed: 21141893]
- [72]. Lamm AN, Garner EB, Dixon DA, Liu S-Y. *Angew. Chem. Int. Ed.* 2011; 50:8157–8160.
- [73]. Liu L, Marwitz AJV, Matthews BW, Liu S-Y. *Angew. Chem. Int. Ed.* 2009; 48:6817–6819.
- [74]. Ulmschneider D, Goubeau J. *Chem. Ber.* 1957; 90:2733–2738.
- [75]. Abbey ER, Zakharov LN, Liu S-Y. *J. Am. Chem. Soc.* 2010; 132:16340–16342. [PubMed: 21043508]
- [76]. Abbey ER, Zakharov LN, Liu S-Y. *J. Am. Chem. Soc.* 2011; 133:11508–11511. [PubMed: 21751771]
- [77]. Campbell PG, Zakharov LN, Grant DJ, Dixon DA, Liu S-Y. *J. Am. Chem. Soc.* 2010; 132:3289–3291. [PubMed: 20214402]
- [78]. Luo W, Zakharov LN, Liu S-Y. *J. Am. Chem. Soc.* 2011; 133:13006–13009. [PubMed: 21786818]
- [79]. Luo W, Campbell PG, Zakharov LN, Liu S-Y. *J. Am. Chem. Soc.* 2011; 133:19326–19329. [PubMed: 22070729]
- [80]. Marwitz AJV, Lamm AN, Zakharov LN, Vasiliu M, Dixon DA, Liu S-Y. *Chem. Sci.* 2012 DOI 10.1039/c1sc00500f.
- [81]. Xu S, Zakharov LN, Liu S-Y. *J. Am. Chem. Soc.* 2011; 133:20152–20155. [PubMed: 22091703]
- [82]. Lepeltier M, Lukoyanova O, Jacobson A, Jeeva S, Perepichka DF. *Chem. Commun.* 2010; 46:7007–7009.
- [83]. Wakamiya A, Mori K, Yamaguchi S. *Angew. Chem. Int. Ed.* 2007; 46:4273–4276.
- [84]. Lukoyanova O, Lepeltier M, Laferrière M, Perepichka DF. *Macromolecules.* 2011; 44:4729–4734.
- [85]. Taniguchi T, Yamaguchi S. *Organometallics.* 2010; 29:5732–5735.
- [86]. Agou T, Kobayashi J, Kawashima T. *Org. Lett.* 2006; 8:2241–2244. [PubMed: 16706496]
- [87]. Agou T, Kobayashi J, Kawashima T. *Chem. Commun.* 2007:3204–3206.
- [88]. Agou T, Sekine M, Kobayashi J, Kawashima T. *Chem. -Eur. J.* 2009; 15:5056–5062. [PubMed: 19326374]
- [89]. Agou T, Sekine M, Kobayashi J, Kawashima T. *Chem. Commun.* 2009:1894–1896.
- [90]. Agou T, Sekine M, Kobayashi J, Kawashima T. *J. Organomet. Chem.* 2009; 694:3833–3836.
- [91]. Agou T, Kojima T, Kobayashi J, Kawashima T. *Org. Lett.* 2009; 11:3534–3537. [PubMed: 19719196]
- [92]. Agou T, Arai H, Kawashima T. *Chem. Lett.* 2010; 39:612–613.

- [93]. Hatakeyama T, Hashimoto S, Seki S, Nakamura M. *J. Am. Chem. Soc.* 2011; 133:18614–18617.  
[PubMed: 22026463]

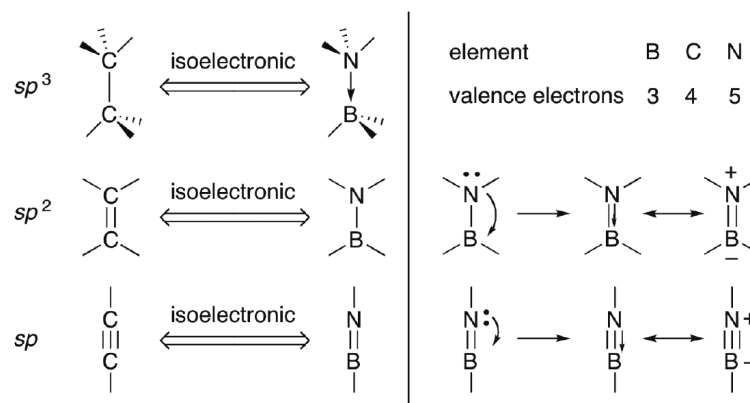


**Figure 1.** Isoelectronic relationship between CC and BN. The notation illustrated on the left column is used throughout this review.

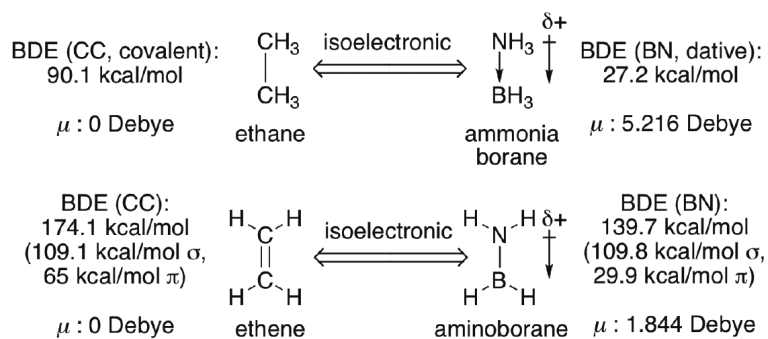


**Figure 2.**  
Molecular consequences of BN/CC isosterism.

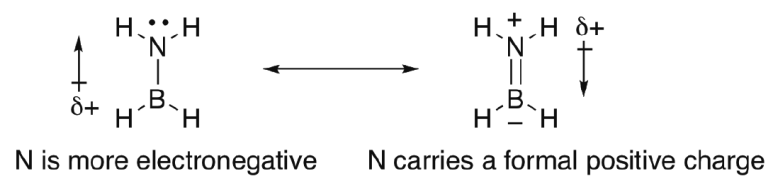


**Figure 3.**  
An intuitive explanation for reduced dipolemoment in aminoborane vs. AB.



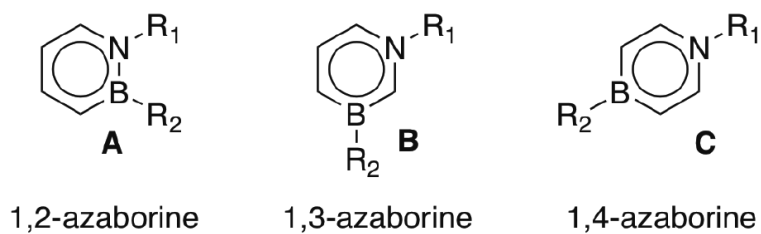


**Figure 4.**  
Isomeric forms of singly substituted aromatic CBN heterocycles

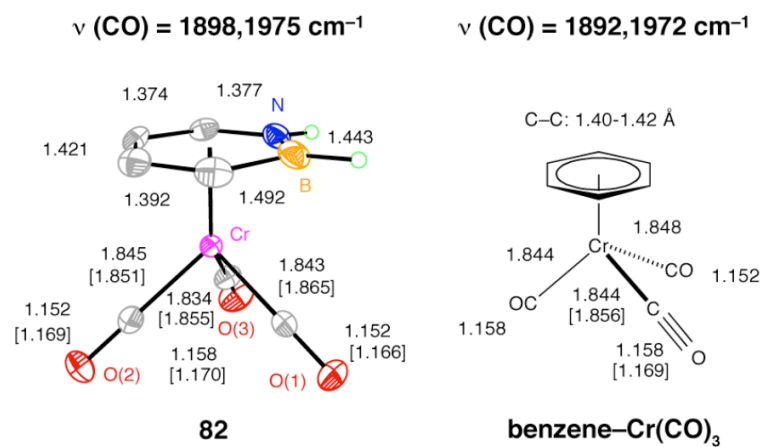
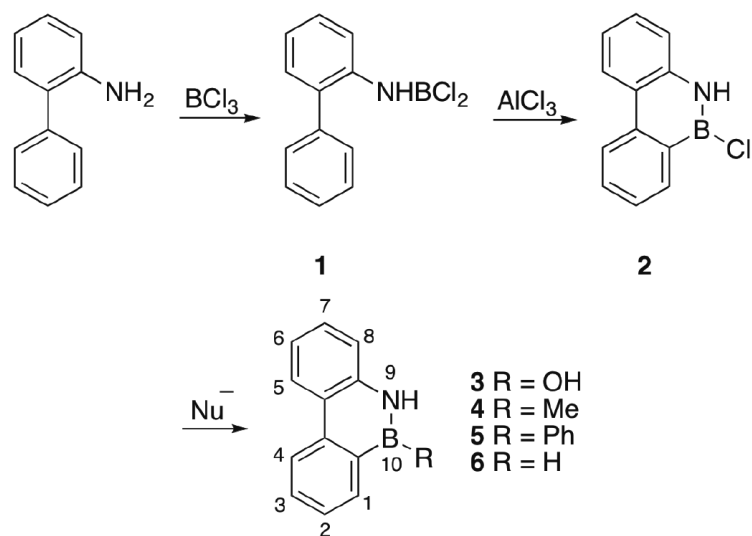
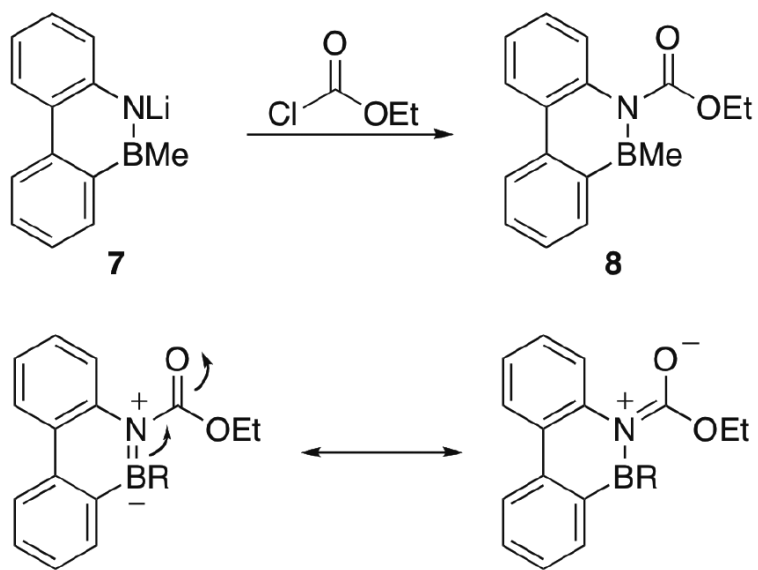


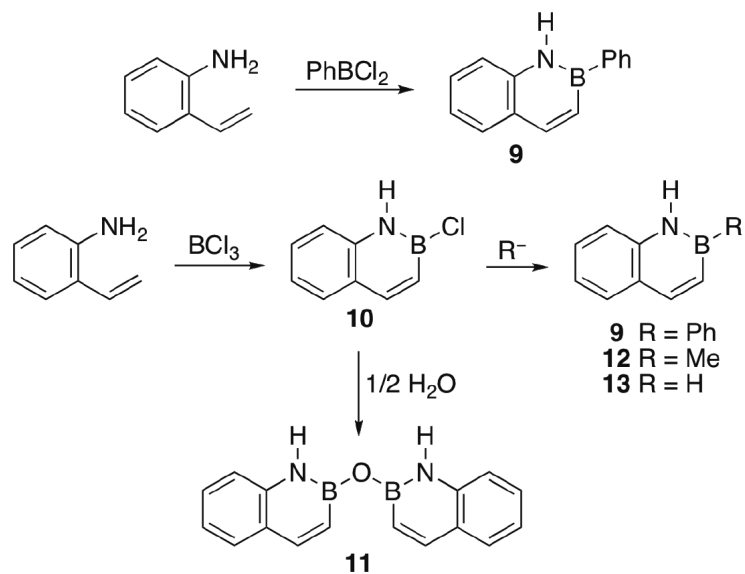
**Figure 5.** Bond lengths (in Å) and carbonyl stretching frequencies for **82** and benzene-Cr(CO)<sub>3</sub>. Computed values are in parentheses.



**Scheme 1.**  
Preparation of boron-substituted 9,10-azaboraphenanthrene derivatives.

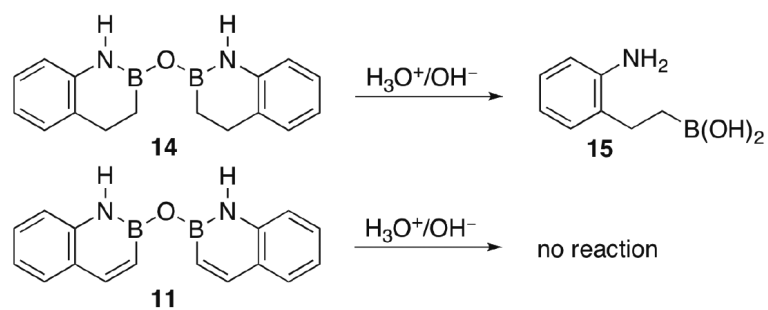


**Scheme 2.**  
Installation of a p-accepting group at the nitrogen of BN-phenanthrene.

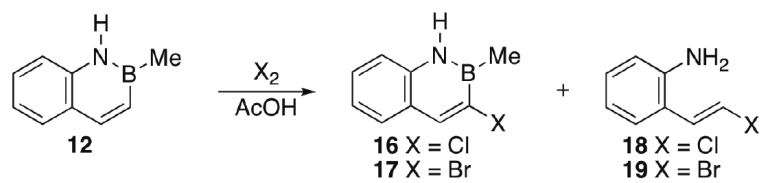


**Scheme 3.**  
Synthesis of B-substituted 1,2-azaboranaphthalenes.

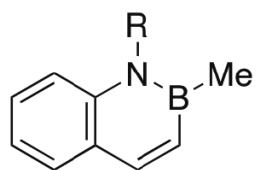




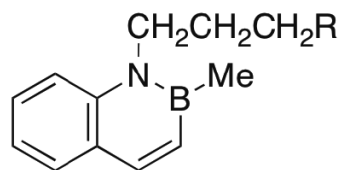
**Scheme 4.**  
Comparison of hydrolytic stability of BN-naphthalene **11** versus reduced anhydride **14**.



**Scheme 5.**  
EAS reactivity of BN-naphthalene **12**.



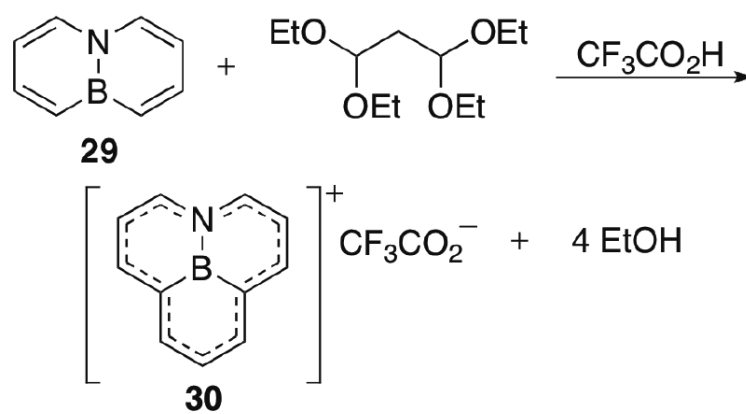
- 12** R = H  
**20** R = Li  
**21** R = CH<sub>2</sub>CH<sub>2</sub>CH<sub>2</sub>Cl  
**27** R = CO<sub>2</sub>Et



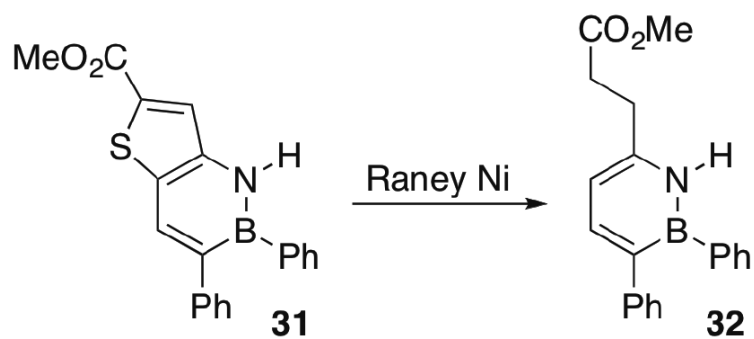
- 22** R = NMe<sub>2</sub>  
**23** R = NEt<sub>2</sub>  
**24** R = piperidino  
**25** R = morpholino  
**26** R = CN

**Scheme 6.**  
Synthesis of water-soluble BN-naphthalenes.

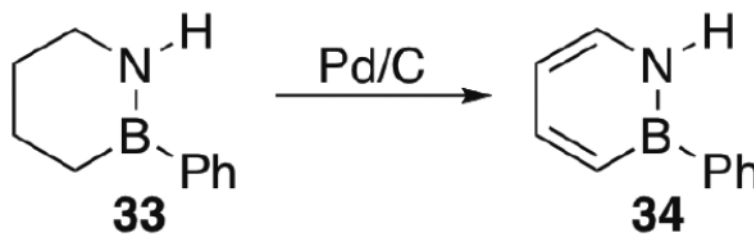




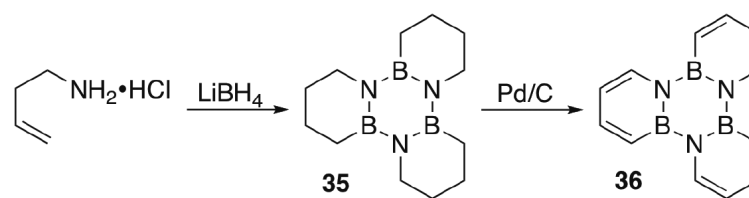
**Scheme 8.**  
Formation of BN-phenalenium cation **30** from BN-naphthalene **29**.

**Scheme 9.**

Synthesis of 1,2-azaborine derivative **32** via desulfurization with Raney nickel (Dewar, 1962).

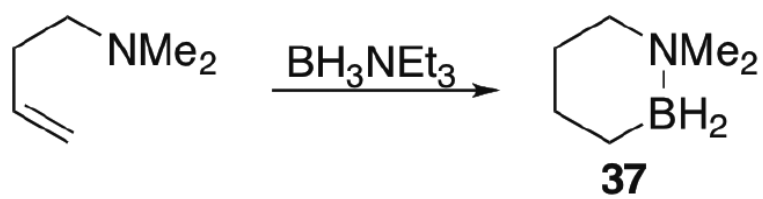


**Scheme 10.**  
Dehydrogenation route to 1,2-azaborine **34** (White, 1963).

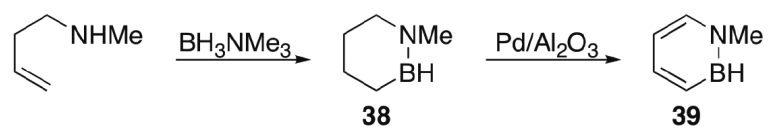


**Scheme 11.**  
Hydroboration-oxidation protocol leading to undesired trimerization to BN-triphenylene **36**.

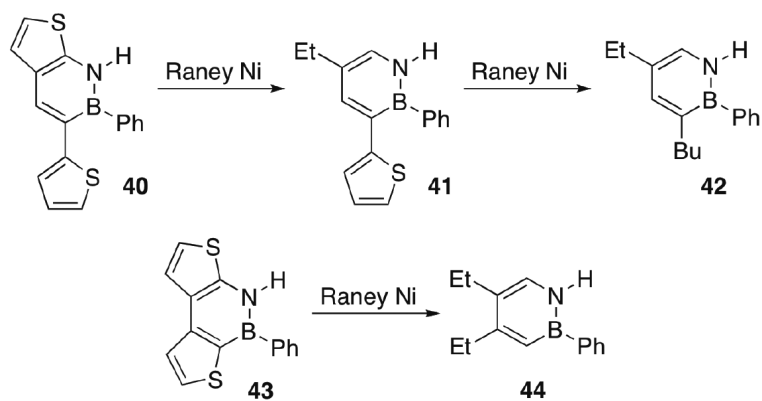




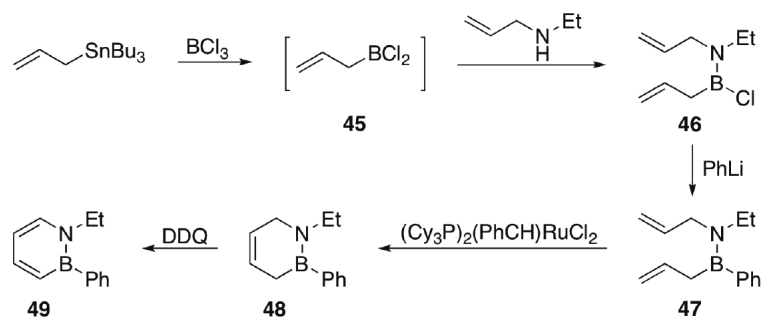
**Scheme 12.**  
Hydroboration to stable 1,2-azaboracyclohexane **37**.

**Scheme 13.**

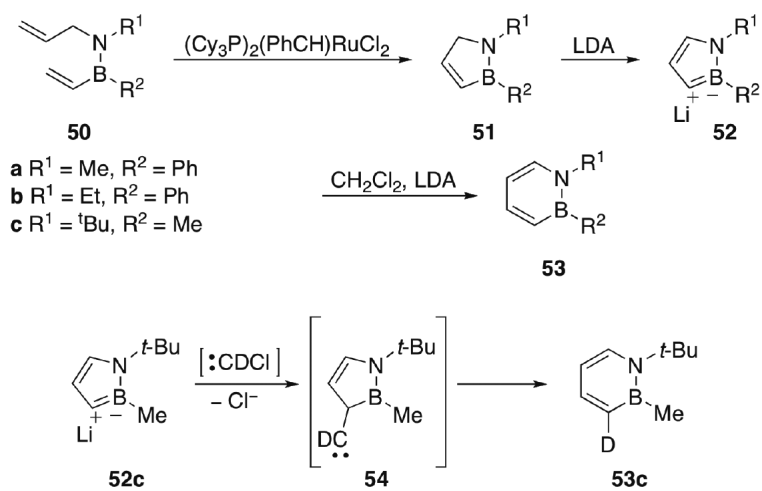
Hydroboration-oxidation to generate B-H substituted 1,2-azaborine **39**.

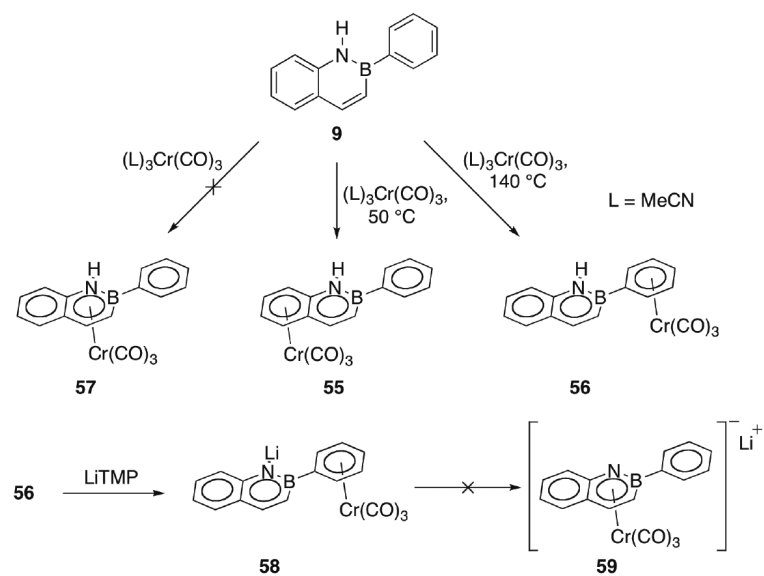
**Scheme 14.**

Desulfurization of BN-benzothiophenes with Raney nickel to generate 4- and 5-substituted 1,2-azaborines.

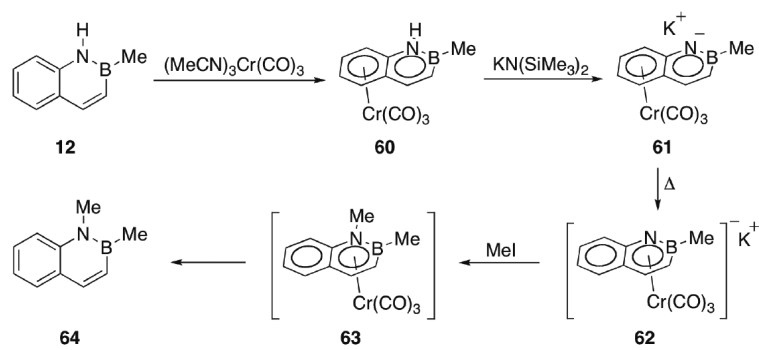


**Scheme 15.**  
Mild synthesis of 1,2-azaborine **49** via ring-closing metathesis.

**Scheme 16.**Ring-expansion route to 1,2-azaborines **53a–c** and deuterium labeling.

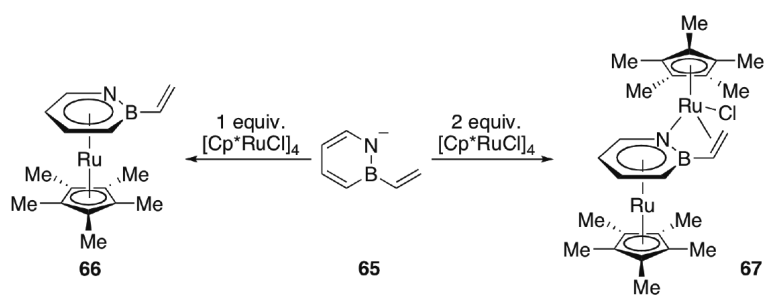


**Scheme 17.**  
Haptotropic migration of Cr-complexes of *B*-phenyl-1,2-azaboranaphthalene **9**.

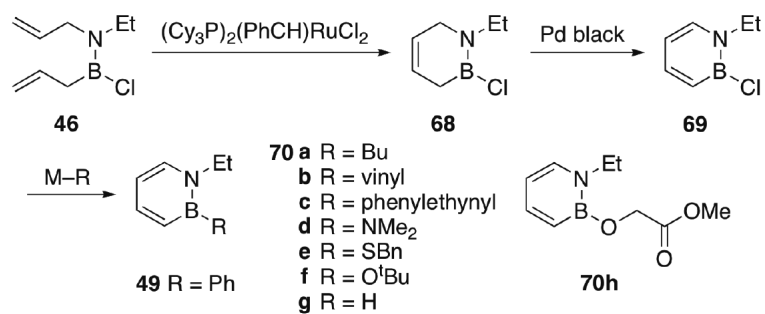


**Scheme 18.**  
Haptotropic migration of Cr-complexes of *B*-methyl-1,2-azaboranaphthalene **12**.

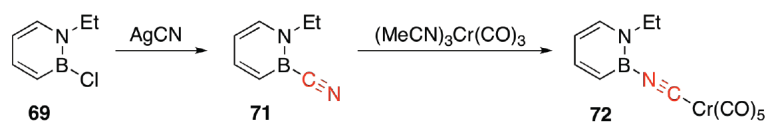




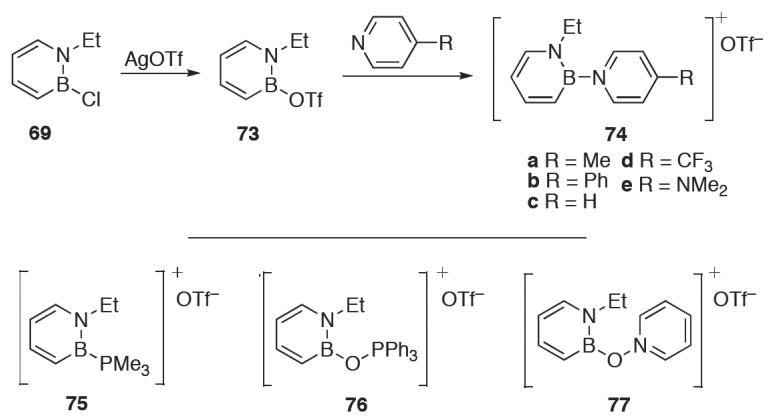
**Scheme 19.**  
Synthesis of complexes **66** and **67** from BN-styrene **65**.



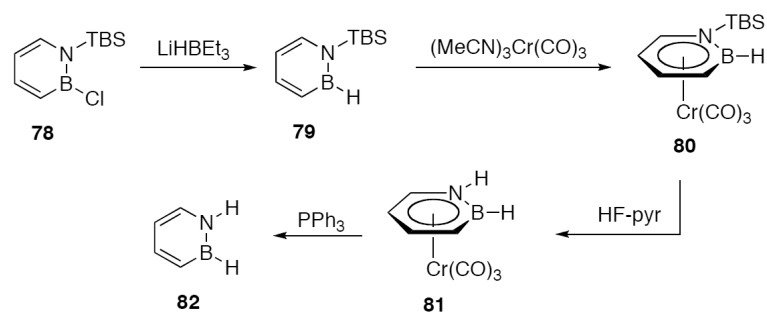
**Scheme 20.**  
Nucleophilic substitution of **69** to generate *B*-substituted 1,2-azaborines.



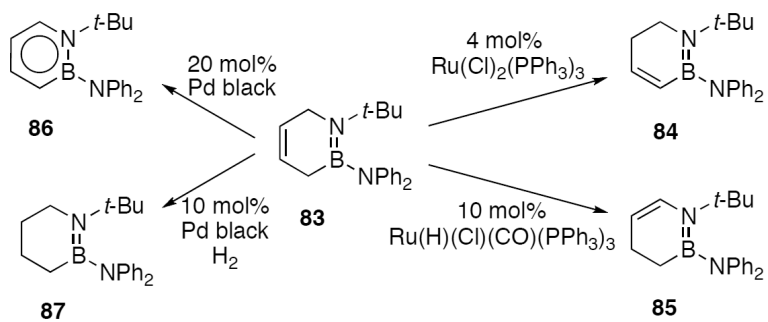
**Scheme 21.**  
Synthesis of BN-benzonitrile and unexpected isomerization to complex **72**.



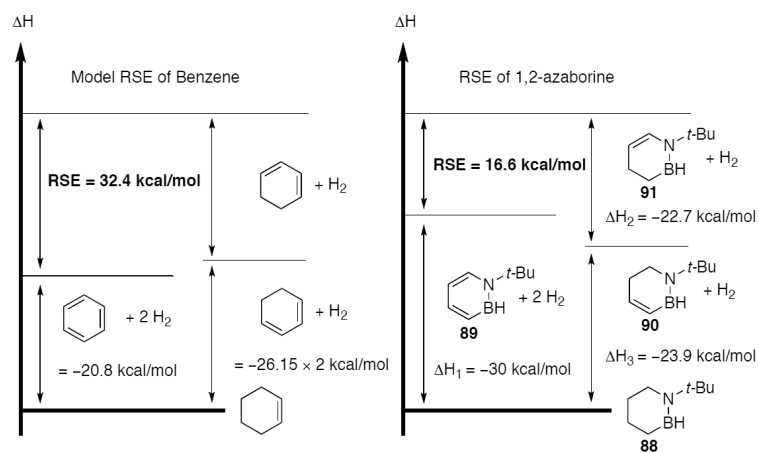
**Scheme 22.**  
Synthesis of 1,2-azaborine cations **74–77**.



**Scheme 23.**  
Synthesis of 1,2-dihydro-1,2-azaborine **82**.

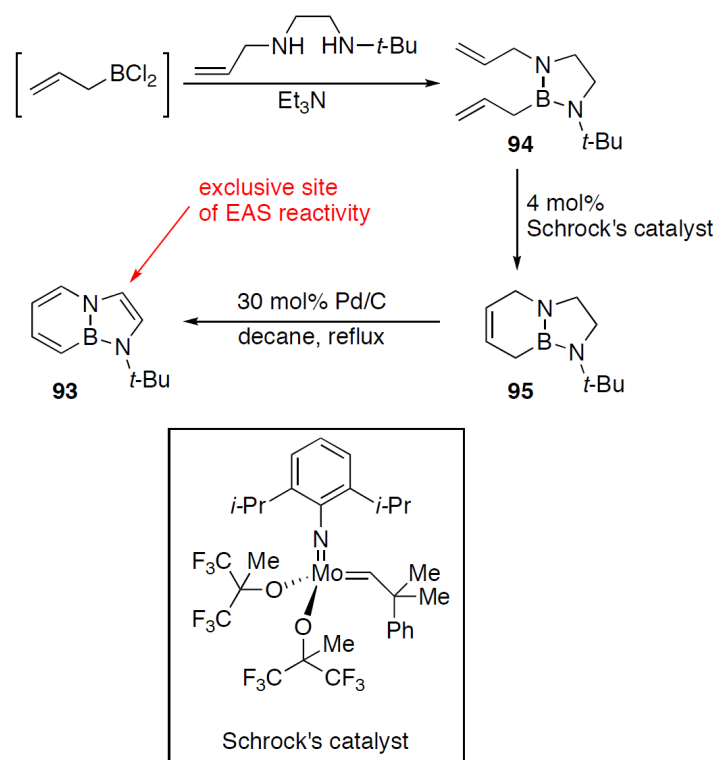
**Scheme 24.**

Catalytic formation of 1,2-azaborine isomers **84–87** from common intermediate **83**.

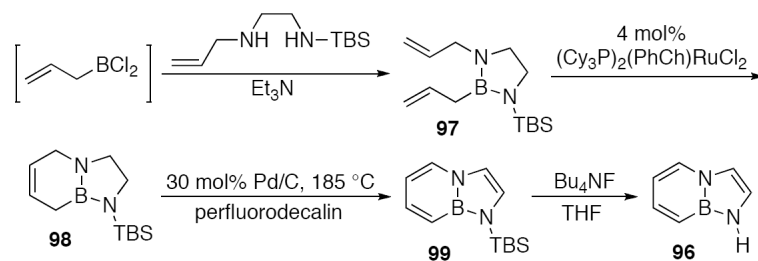
**Scheme 25.**

Experimentally determined resonance stabilization energy of 1,2-azaborine.

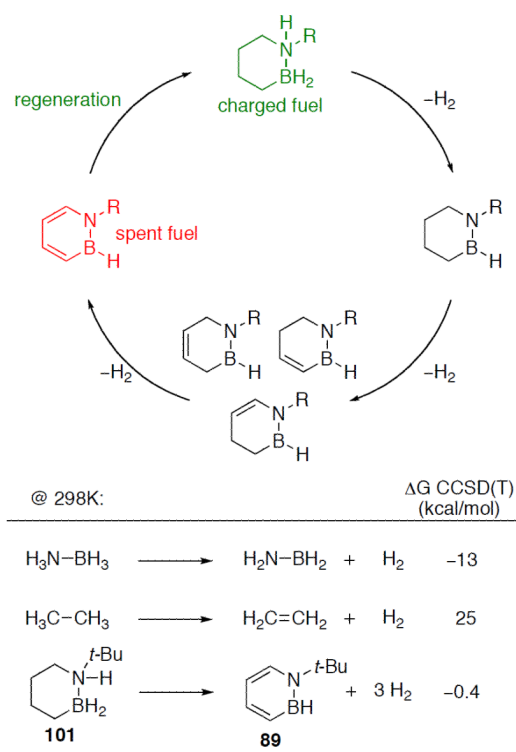




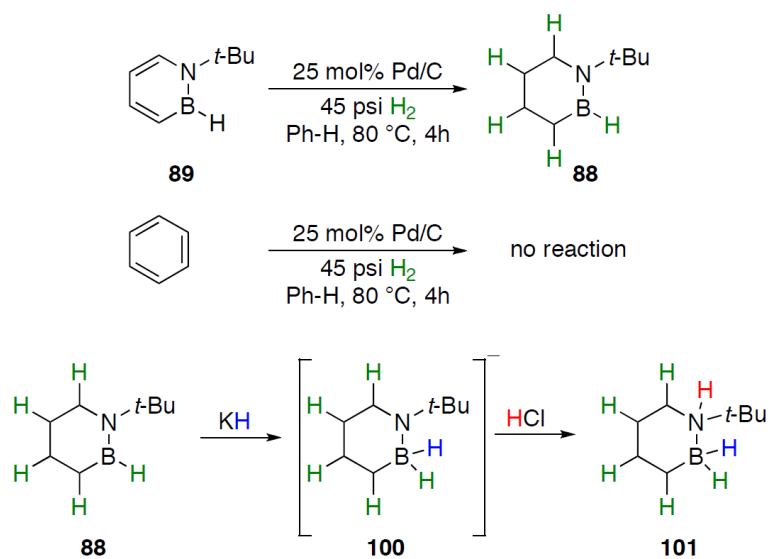
**Scheme 26.**  
Synthesis of *N*-*t*-Bu-BN-indole **93**.



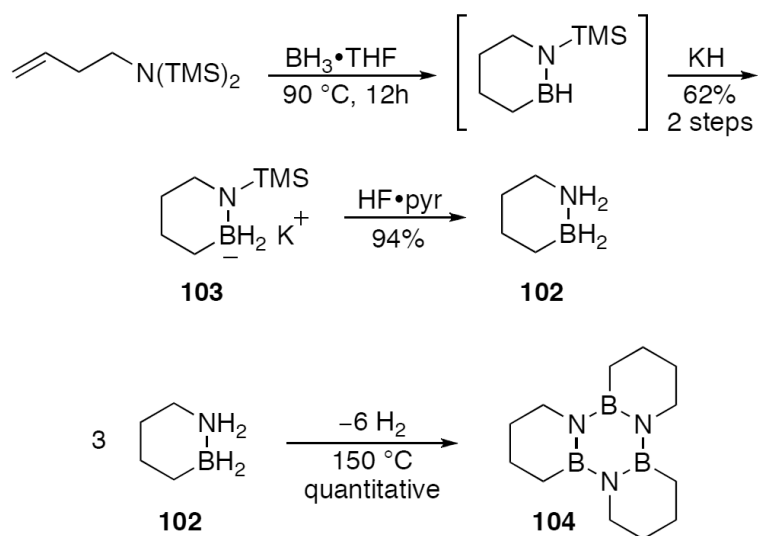
**Scheme 27.**  
Synthesis of the parent "fused" BN-indole **96**.



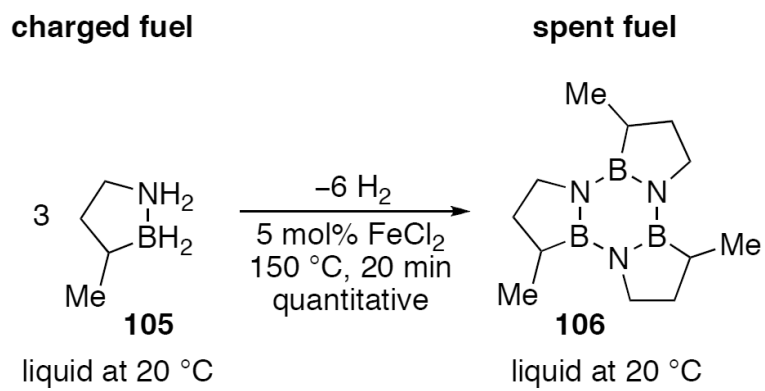
**Scheme 28.**  
Hydrogen storage by CBN heterocycles.

**Scheme 29.**

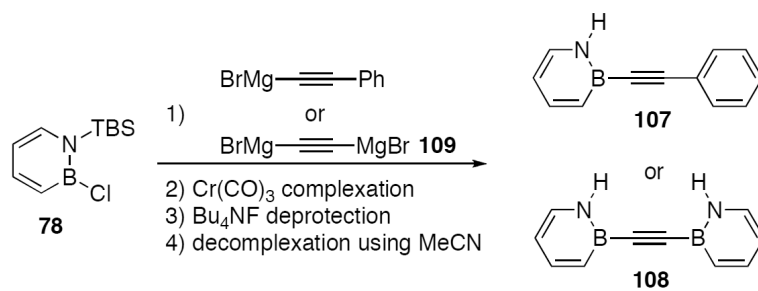
Regeneration of 1,2-azaborine spent fuel **89** via catalytic hydrogenation of C=C bonds and sequential addition of H<sup>-</sup>/H<sup>+</sup> across the B–N bond.

**Scheme 30.**

Synthetic route to 1,2-azaboracyclohexane **102** and dehydrogenation/trimerization to form **104**.

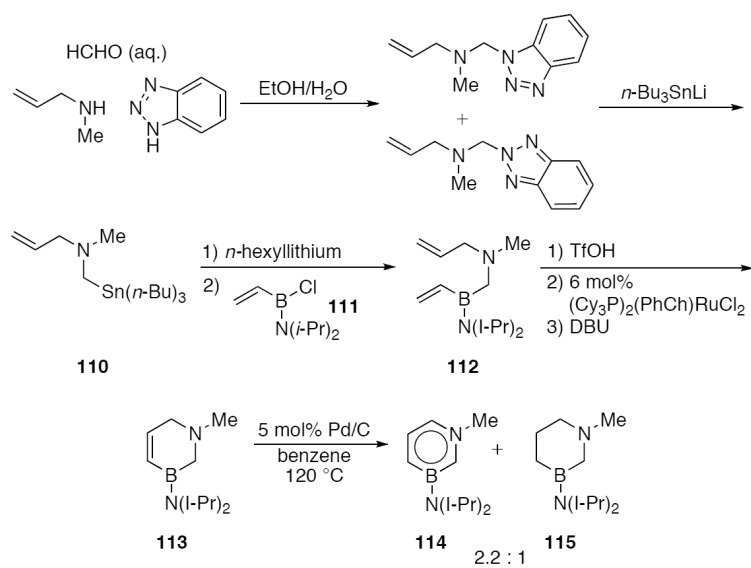


**Scheme 31.**  
Liquid hydrogen storage material based on BN-methylcyclopentane **105**.

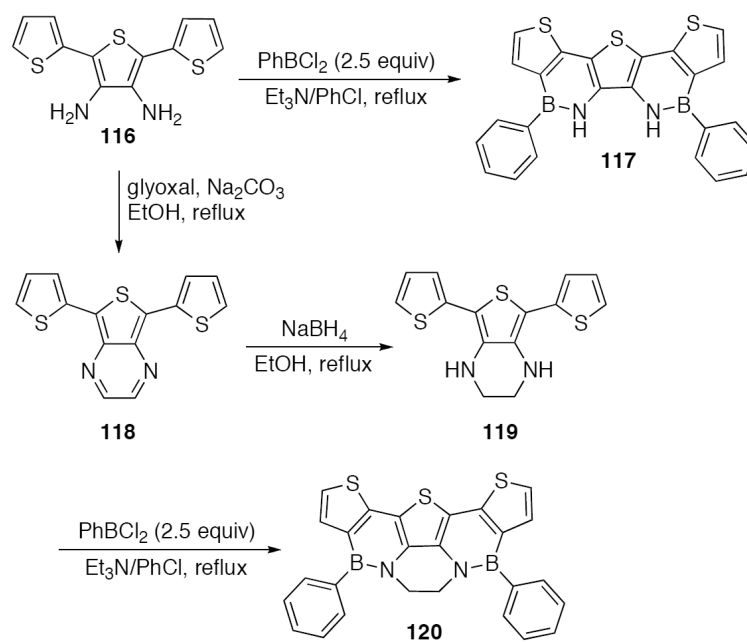


**Scheme 32.**  
Synthesis of BN-tolan analogs **107** and **108**.

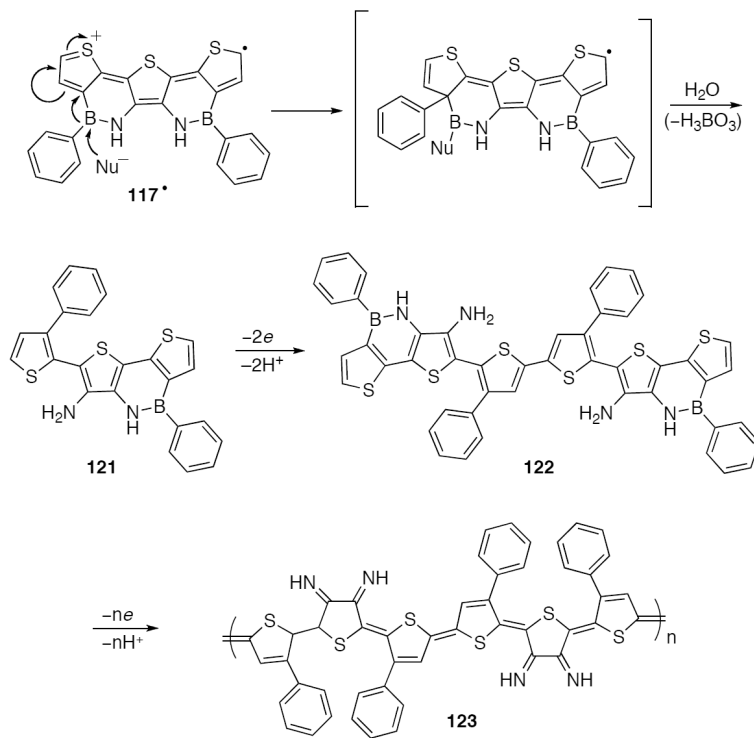




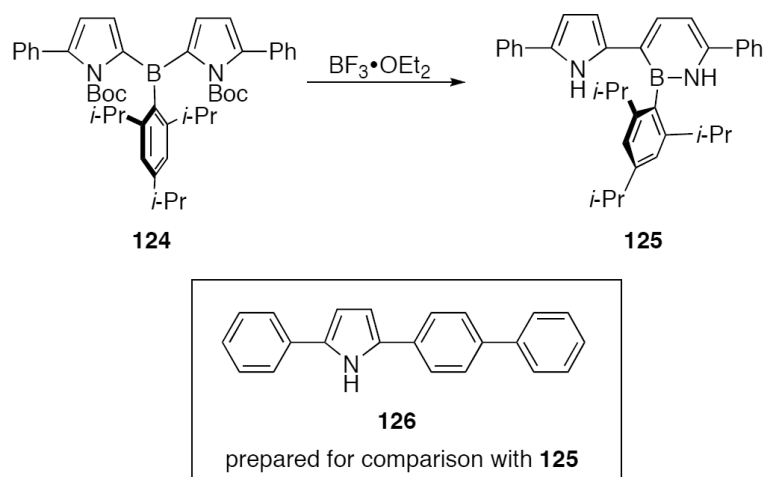
**Scheme 33.**  
Synthesis of the first 1,3-azaborine **114**.



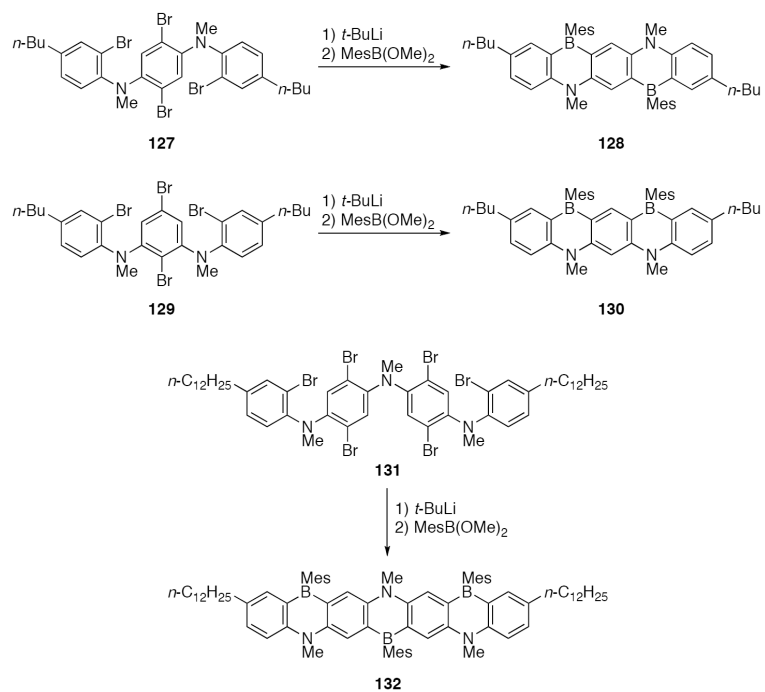
**Scheme 34.**  
Synthesis of 1,2-azaborine-fused oligothiophene materials **117** and **120**.



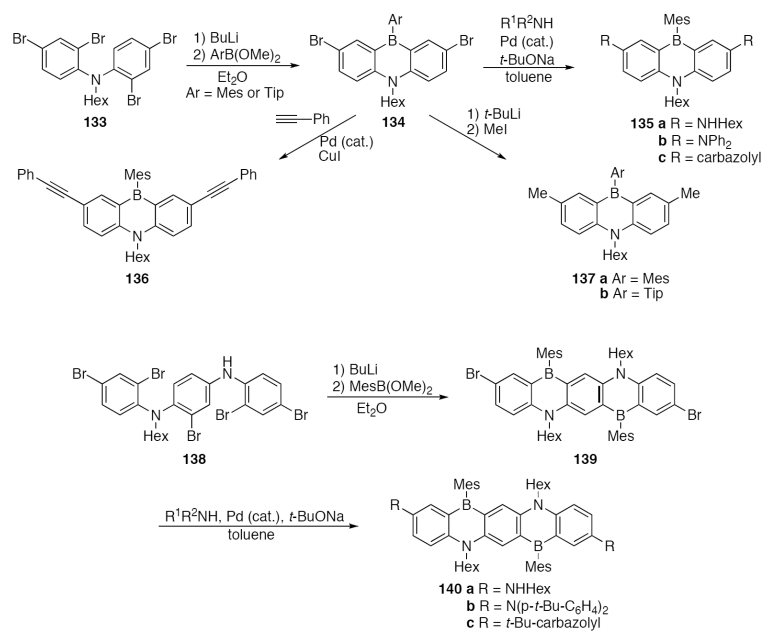
**Scheme 35.**  
Proposed formation of deborylated polymer **123** from **117** via intermediates **121** and **122**.



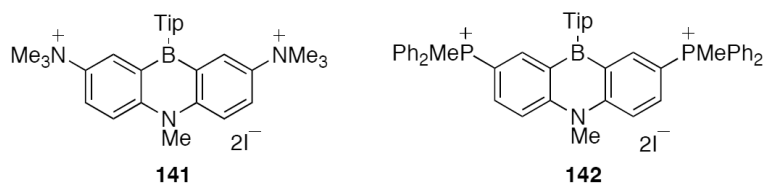
**Scheme 36.**  
Synthesis of  $\Pi$ -conjugated 1,2-azaborine material **125**.



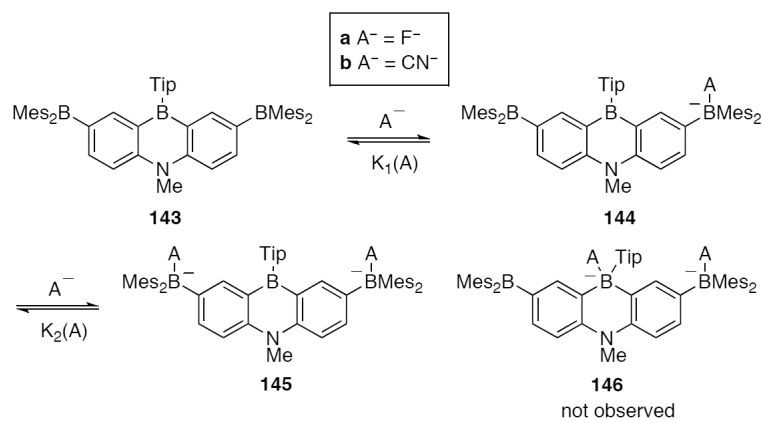
**Scheme 37.**  
 Synthesis of BN-pentacene isomers **123** and **125** and BN-heptacene **127**.



**Scheme 38.**  
 General route to BN-anthracenes **135–137** and BN-pentacenes **140a–c**.

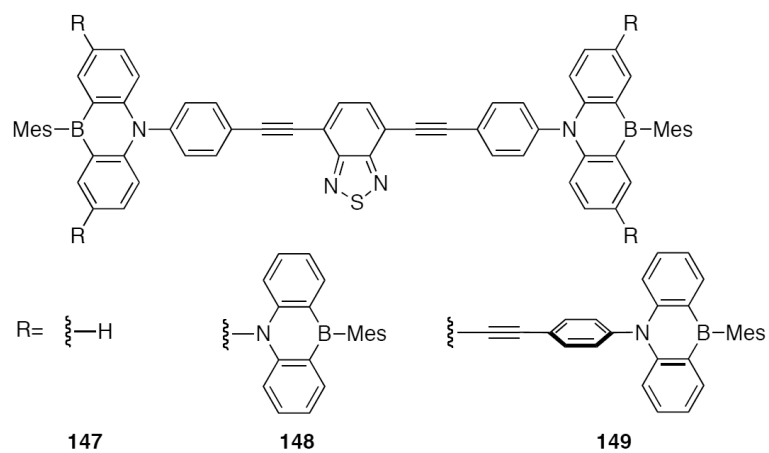


**Scheme 39.**  
Dicationic BN-anthracenes **141** and **142**.



**Scheme 40.**  
 Multistep  $F^-$  and  $CN^-$  anion sensing with bis(dimesitylboryl)azaborine **143**.

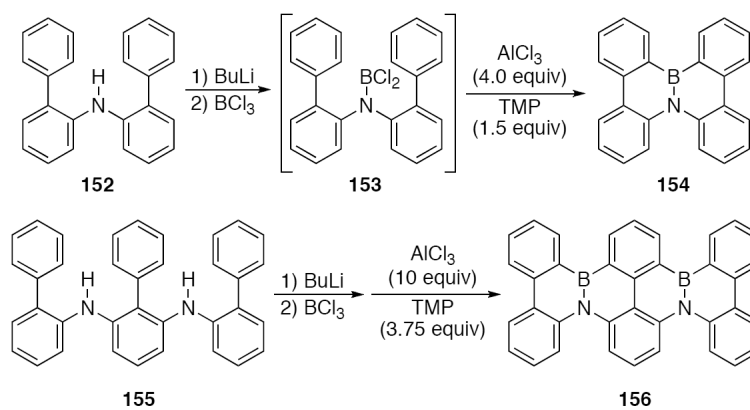




**Scheme 41.**  
 $\Pi$ -conjugated dendrimers based on BN-anthracene.

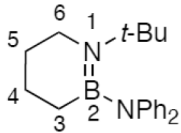
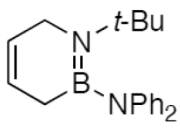
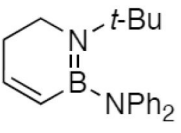
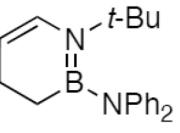
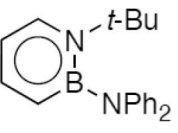


**Scheme 42.**  
Synthesis of dinaphthoazaborine **151**.

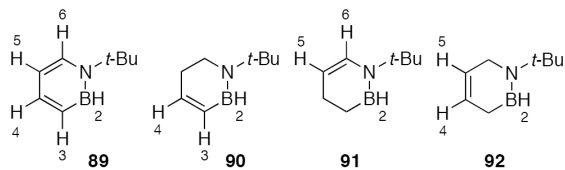


**Scheme 43.**  
Synthesis of BN-fused polyaromatics **154** and **156**.

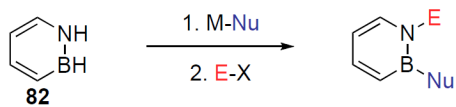
**Table 1**Selected Bond Distances and Deviations from Planarity (Å) for Heterocycles **83–87**.

					
	<b>87</b>	<b>83</b>	<b>84</b>	<b>85</b>	<b>86</b>
B–N <sub>ring</sub>	1.403(2)	1.405(2)	1.407(2)	1.417(3)	1.446(2)
B–C <sub>3</sub>	1.584(3)	1.590(2)	1.559(2)	1.579(4)	1.518(2)
C <sub>3</sub> –C <sub>4</sub>	1.511(3)	1.493(2)	1.338(2)	1.504(4)	1.363(2)
C <sub>4</sub> –C <sub>5</sub>	1.511(3)	1.319(2)	1.479(2)	1.494(4)	1.412(2)
C <sub>5</sub> –C <sub>6</sub>	1.508(3)	1.493(2)	1.503(2)	1.319(3)	1.356(2)
C <sub>6</sub> –N <sub>ring</sub>	1.479(2)	1.477(2)	1.479(2)	1.432(3)	1.383(2)
B–N <sub>exo</sub>	1.488(2)	1.478(2)	1.483(2)	1.480(3)	1.486(2)
planarity <sup>a</sup>	0.226	0.164	0.199	0.183	0.048

<sup>a</sup>Root mean square deviation of intra-ring atoms from least-squares plane (in Å).

**Table 2**Downfield  $^1\text{H}$  chemical shift as 1,2-azaborine becomes aromatic.

	<b>89</b>	<b>90</b>	<b>91</b>	<b>92</b>	<b><math>\Delta\delta</math> downfield</b>
$\text{H}_{\text{B}(2)} \delta$ :	5.23	4.45	4.91	4.75	0.78, 0.32, 0.48
$\text{H}_{\text{C}(3)} \delta$ :	6.84	5.91			0.93
$\text{H}_{\text{C}(4)} \delta$ :	7.54	6.55		5.71	0.99, 1.83
$\text{H}_{\text{C}(5)} \delta$ :	6.38		5.02	5.62	1.36, 0.76
$\text{H}_{\text{C}(6)} \delta$ :	7.63		6.21		1.42

**Table 3**Substrate scope of nucleophilic aromatic substitution of **82**.

Entry	M-Nu	E-X	Yield (%) <sup>a</sup>
1	Na-O <i>t</i> -Bu	H-Cl	63
2	K-Oallyl	H-Cl	79
3	Li- <i>t</i> -Bu	H-Cl	81
4	Li- <i>n</i> -Bu	H-Cl	80
5	Li-Ph	H-Cl	98
6	BrMg-vinyl	H-Cl	59
7	BrMg—≡—Ph	H-Cl	71
8	Li- <i>n</i> -Bu	TMS-Cl	89
9	Li- <i>n</i> -Bu	Me-I	67
10	Li- <i>n</i> -Bu	Bn-Br	60

<sup>a</sup> Isolated yield

**Table 4**

Photophysical properties of BN-acenes.

compound	$\lambda_{\max}$ (nm) / log ( $\epsilon$ )	$\lambda_{\text{em}}$ (nm)	$\Phi$
127	523 / 4.23	534	0.69
130	415 / 3.94	428	0.21
132	608 / 4.28	625	0.55